UNIVERSITÀ' DEGLI STUDI DI TRIESTE

XXV CICLO DEL DOTTORATO DI RICERCA IN NANOTECNOLOGIA

Nanotechnology Applications in Quantitative Neuroscience: Proteomic Analysis of Malignant Gliomas

Settore Disciplinare: FIS/03

DOTTORANDO
Mario Ganau

COORDINATORE
Prof Maurizio Fermeglia

SUPERVISORE DI TESI
Prof Giacinto Scoles

TUTOR
Dott.ssa Loredana Casalis

ANNO ACCADEMICO 2011 / 2012

To all those who constantly supported me
during those challenging years

Nanotechnology Applications in Quantitative Neuroscience: Proteomic Analysis of Malignant Gliomas

Outline

Abstract (En)

The current limit of knowledge advancement in proteomic analysis of gliomas, the most common primary malignant brain tumors, is related to the high sensitivity required to detect specific biomarkers within few cells volumes. To address this problem we developed a quantitative approach to eventually enable precise, high throughput and low cost analysis of glial cells with potential capability of real-time pathological screening and subtyping of brain tumors.

A device consisting in micro-fabricated wells capable to isolate and host living astrocytes was designed and functionalized. Then for the fabrication of a nanobiosensor, able to detect in small volumes the presence of specific biomarkers, ideally for multiplexing assays and meant to fit within the small dimensions of this microdevice, an approach consisting in DNA-directed-immobilization (DDI) of biotinylated antibodies (Abs) on a single stranded DNA (ssDNA) nanoarray, produced by Atomic Force Microscopy (AFM) nanografting, was carefully optimized. The proof of concept was realized with Abs specific for Glial Fibrillary Acidic Protein (GFAP), a biomarker which belongs to the family of intermediate filaments and is crucial in cell's differentiation, within a platform ready for parallelization.

Nanosized patches of thiol modified ssDNA were prepared by AFM-based nanografting inside a matrix of self assembled monolayers (SAM) of alkanethiol-modified gold surfaces. Subsequently a complementary DNA strand (cDNA) conjugated to streptavidin (STV) was allowed to covalently bind to the patch by sequence specific DNA hybridization. Finally the biotin binding sites of STV were exploited to immobilize biotinylated monoclonal GFAP Abs (already in use for ELISA assays) on the top of those nanopatches. The efficiency of those nano-immuno arrays was tested by successfully obtaining the immobilization of purified recombinant GFAP protein, down to a concentration of 4 nM, firstly in standard PBS then in multicells' lysate obtained from U87 glial cultures. The immobilization was detected by means of AFM measuring step by step the increases in the height of the patches and excluding modification of the roughness of both the SAM and the nanopatches after incubation with the cells' lysate through a signal to noise ratio analysis. Titration curves for a comparison of sensitivity between this technique and the conventional ELISA assays are provided; they indeed confirm that the sensitivity of our nanosensors is at least that of ELISA, with the advantage of the scalability of the device.

Abstract (It)

L'attuale limite di avanzamento dello stato dell'arte dell'analisi proteomica dei gliomi cerebrali, la classe istologica di tumori cerebrali più frequente ed aggressiva, è legato alla difficoltà di individuare specifici biomarkers in piccoli volumi cellulari. Per superare questo limite si è deciso di sviluppare un approccio nanoquantitativo che consenta un'analisi proteomica precisa, ad alta sensibilità e basso costo, degli astrociti tumorali, con potenzialità di screening in tempo reale e sottotipizzazione di tumori cerebrali. Previa fabbricazione e funzionalizzazione di micro pozzetti idonei ad ospitare cellule astrocitarie, ci si è dedicati alla realizzazione di biosensori in grado di riconoscere specifici biomarkers e di essere accoppiati ai micro pozzetti. Al fine di immobilizzare anticorpi specifici per proteine di interesse in ambito neuroncologico, è stato scelto un approccio basato sul nanografting con Microscopio a Forza Atomica (AFM) e sull'immobilizzazione diretta sul DNA di anticorpi (DDI). In particolare la prova concettuale è stata condotta con anticorpi specifici per la Glial Fibrillary Acidic Protein (GFAP), un marcatore della differenziazione astrocitaria appartenente alla famiglia dei filamenti intermedi intracellulari, su una piattaforma atta ad una successiva parallelizzazione.

I nanocostrutti responsabili del riconoscimento della proteina d'interesse, sono stati realizzati partendo da molecole di DNA a singola elica (ssDNA) graftate in una matrice di monostrati autoassemblati (SAM) di superfici d'oro alchiltiolo modificato. Al fine di sfruttare la capacità della streptavidina (STV) di legarsi ad anticorpi biotinilati è stata successivamente indotta l'ibridazione di un filamento di DNA complementare (cDNA) a quello precedentemente immobilizzato sulla superficie nanoassemblata che presentasse anche una coda di STV. I siti di legame per la biotina intrinseci al tetramero di STV sono quindi stati sfruttati per immobilizzare sulla superficie dei nanocostrutti degli anticorpi monoclonali biotinilati specifici per GFAP (già in uso per i protocolli ELISA). L'efficienza dei nano-immuno costrutti così ottenuti è stata testata ottenendo l'immobilizzazione di GFAP ricombinante anche a basse concentrazioni (fino a 4nM), sia in presenza di standard PBS, sia in presenza di un lisato multicellulare ottenuto da colture gliali di cellule U87. L'immobilizzazione di GFAP è stata confermata dall'incremento in altezza dei nanocostrutti misurato all'AFM escludendo modificazioni del rapporto segnale/rumore sia del SAM che dei nanocostrutti prima e dopo aggiunta di lisato multicellulare. Il limite di sensibilità del prototipo così ottenuto è stato confrontato con quello raggiungibile con protocolli standard ELISA, mostrando una sensibilità almeno comparabile all'ELISA a fronte di un maggiore potenziale diagnostico legato alla sua scalabilità.

Acknowledgements

My sincere and infinite gratitude goes to my supervisor Prof Giacinto Scoles and my tutor Dr Loredana Casalis because by accepting me in their laboratory three years ago, they gave me a precious, once in a lifetime opportunity. Their enormous encouragement and genuine help made me feeling comfortable in such a technical nano-world, so far away from my clinical-surgical daily practice.

I would like to express my deepest thanks to Dr Alessandro Bosco, Dr Pietro Parisse, Dr Barbara Sanavio and Dr Denis Scaini for their passionate help in teaching me the fundamentals of AFM and nanografting process. All those fruitful hours spent together contributed to increase my understanding of the complexity surrounding proteomic assays. Indeed, they have been invaluable in helping me to overcome the many unsuccessful experiments and to keep progressing towards the optimization of the most convenient strategy for nano-immobilization of proteins.

My huge appreciation goes to my colleagues at the NanoInnovation Lab, Stefania Corvaglia, Luca Ianeselli and Maryse Nkoua who cared about supporting me in several parallel procedures carried out during this PhD project, and for offering me their excellent skills during hard tasks such as the microwells fabrication and their effective functionalization. As well I would like to thank Anita Palma for her precious efforts to enabling an effective comparison in terms of sensitivity between our methodology and the standard ELISA assays.

I would like to thank Dr Daniela Cesselli for the thorough encouragement and meaningful discussions on single cells proteomics and its correlation with practical pathological needs, her expert guidance helped us in understanding the potentialities of the device developed in those years and formed the basis for its further clinical characterization.

I am also particularly thankful to all those that enabled a tight collaboration with the partner labs where some experiments have been realized or part of them made possible: the IOM INFM @ TASC for the support provided in the fabrication of microwells, the Structural Biology Lab @ Elettra and Spinal Biophysics Lab @ UniTS for the opportunity to test living prokaryotes and eukaryotes within the microwells, and the Dept of Medical and Biological Sciences @ UniUD for the benchmark testing with ELISA protocols.

Finally, I am immensely grateful to my fiancée Lara, my parents Francesco and Marinella and my sister Laura for their endless love, enduring support and constant guidance during those long and fruitful years here in Trieste.

Chapter 1:

Introduction

1.1 Background

Based upon the latest genetic and proteomic insights into cancer' biology, which opened new avenues for novel applied clinical research, trends in oncology highlight that molecular characterization of the tumorigenesis process will be essential in tomorrow's clinical practice to predict prognosis and guide therapy. Noteworthy, the promise of individualized molecular medicine, which is particularly relevant to oncology because even similarly classified tumors can follow quite different clinical outcomes, could be realized by identifying molecular targets for therapy and by measuring tangible response or regression in clinical trials.

Specific patterns of protein expression in tumors and matched normal tissues can now be reliably analyzed using quantitative proteomic techniques. Among them the most effective are enzyme-linked immunosorbent assay (ELISA), two-dimensional gel electrophoresis (2DGE) and matrix-assisted laser desorption ionization time of flight (MALDI-TOF) mass spectrometry, which allow to simultaneously identify and characterize differentially expressed proteins. Nevertheless, arrays of proteins with well-defined feature size and spacing already demonstrated the potential to boost the detection of key biomolecules by favoring the study of surface-cellular interaction. In fact among the current limits of knowledge advancement in oncology the main one is probably related to the high sensitivity required to accurately monitor protein-protein interactions, which are relevant to follow changes in cellular pathways due to different kinds of external perturbations. Such caveat explain why a new quantitative approach based on the nano-immuno-arrays technology, could be highly effective in enabling a precise, high throughput and low cost *in vitro* analysis of tumor cells' lysates, or *in vivo* studies of their secretome (down to the single cells level).

Focusing our attention to neuro-oncology we identified the remarkable need for more sophisticated diagnostic tools with potential capability of real-time pathological screening and subtyping of glial tumors.

1.2 Gliomas

Gliomas (see Fig 1.1) are primary brain tumors classified according to the histological classification of the World Health Organization in: Glioblastomas (Grade IV), Anaplastic Astrocytomas (Grade III), Low Grade Astrocytomas and Oligodendrogliomas (Grade II). Among them the most aggressive ones, namely Glioblastomas and Anaplastic Astrocytomas present an incidence of 3.5-2.8 and 0.3-1.2 new cases per 100.000 per year respectively (Ohgaki et al, 2005; Deorah et al, 2006).

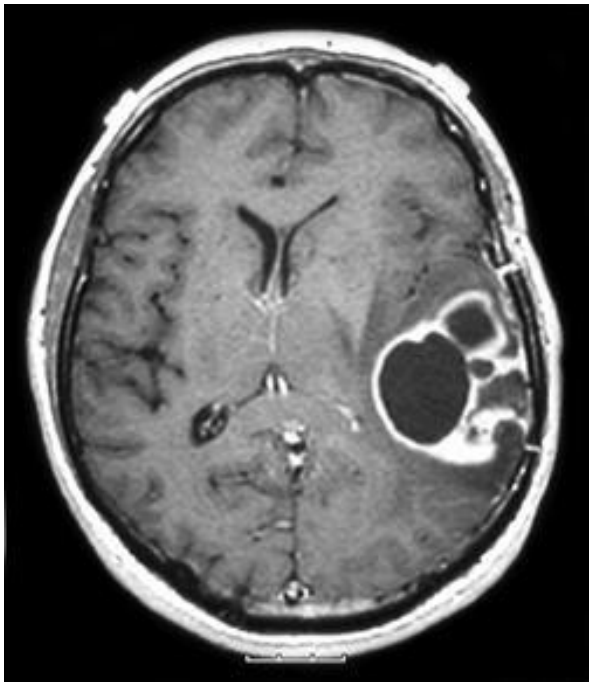

Fig 1.1: T1-weighted MRI image showing a left temporal high-grade glioma

Gliomas are characterized by rapid growth, high level of cellular heterogeneity (see Fig 1.2) due to genetic alteration, and infiltrative behaviour, nevertheless those tumors are generally confined in the brain parenchyma, and do not show any tendency to bony calvarium or extracranial invasion. It is recognized that more complete resections lead to better prognosis, accordingly microscopic local resection is the current neurosurgical end point. Despite that, tumor infiltration is unfortunately widespread and recurrence may occur near resection margin as well as far away from it in both cerebral hemispheres, rarely in the cerebellum and even more rarely in the spinal cord.

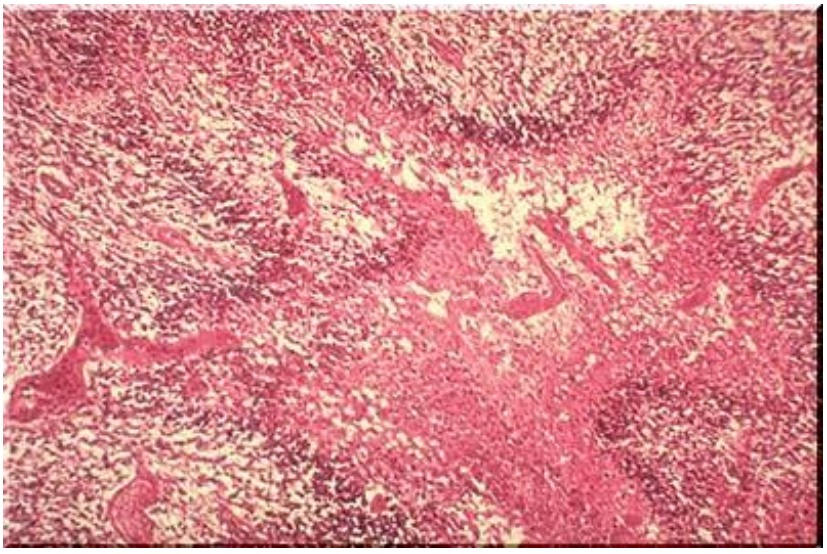

Fig 1.2: Hematoxylin and eosin stain of a high-grade glioma showing the high degree of cellularity and neovascularisation, typical features of those tumors

Radiotherapy is therefore central in the treatment of high grade gliomas, since limited field fractionated radiation, covering the MRI enhanced lesion as well as peritumoral edema, improves patients survival: the standard dose is 60 Gy (Fine et al, 1993).

Temozolomide (TMZ) received Food and Drug Administration approval in 1999 for refractory Anaplastic Astrocytomas, followed by the first line indication for Glioblastoma. The international EORTC/NCIC trial in 2005 demonstrated a substantial improvement in median survival, representing the first of such improvements since the introduction of radiation therapy in the mid-1970s (Stupp et al, 2005). Local intraoperative therapy with antineoplastic wafers (impregnated carmustine implants) has demonstrated a further survival advantage although only in patients with O(6)-methylguanine-DNA methyltransferase (MGMT) promoter methylation (Westphal et al, 2003; Lechapt-Zalcman et al, 2012).

To date, complete microscopic excision followed by adjuvant radio- or chemotherapy represents the standard of care, nevertheless tumor recurrence generally occurs within few months due to the widespread neoplastic infiltration (Smoll et al, 2012). In fact, primary brain tumors invade widely spreading single cells anywhere within the brain parenchyma, through infiltration of blood vessel walls, subpial glial spaces, or white matter tracts. These mechanisms lead to the development of tumor satellites that escape resection and treatment, eventually serving as reservoirs for tumor recurrences. Beside parenchymal infiltration, another challenge in the management of gliomas is the nearly universal propensity of these neoplasms to present an intratumoral and intertumoral molecular heterogeneity allowing tumoral reservoirs to be even more resistent to further treatment than the primary lesion (Furnari et al, 2007).

Despite continuous refinements in therapeutic strategies, the prognosis for patients with high-grade gliomas remains dismal, and second-time surgical resection along with local intraoperative positioning of antineoplastic wafers represent the only treatment choices for patients with recurrent gliomas (Westphal et al, 2003). As a result, the median survival of high-grade gliomas is 14-month for patients undergoing surgery plus chemotherapy, and 22-month for those treated with surgery plus chemotherapy plus carmustine wafers; so that only 2.2% of patients are expected to survive 3 years or more after diagnosis of a Glioblastoma (Ohgaki et al, 2005; Smoll et al, 2012).

1.3 GFAP

At present, gliomas are diagnosed by histopathological criteria, and known robust prognostic factors for most of these tumors are limited to tumor grade and patient age.

While there has been progress in understanding some clinical aspects of these tumors (Prados and Levin, 2000; Kitange et al, 2003), new molecular markers are required to better define prognosis and response to therapy

The widespread acceptance that genetic signatures such as losses on chromosomes 1p and 19q are of prognostic value in Oligodendrogliomas (Cairncross et al., 1998) has spurred interest in developing molecular markers to predict outcome and response to treatment across a broader population of gliomas. In fact, while numerous genetic alterations have been described in Glioblastomas (von Deimling et al, 1995; Watanabe et al, 1996), such markers have proved to be of marginal utility in predicting outcome or guiding decisions about disease management.

Importantly, recent expression profiling studies have revealed that proteomic patterns could be of prognostic value (Freije et al, 2004; Nutt et al, 2003), and a systematic review of multiple independent proteomic analyses of gliomas published on PubMed since 2008 has demonstrated alterations of almost 100 different proteins. Among them we have chosen the Glial Fibrillary Acidic Protein (GFAP), a biomarker belonging to the family of intermediate filaments (IF) for our proof of concept.

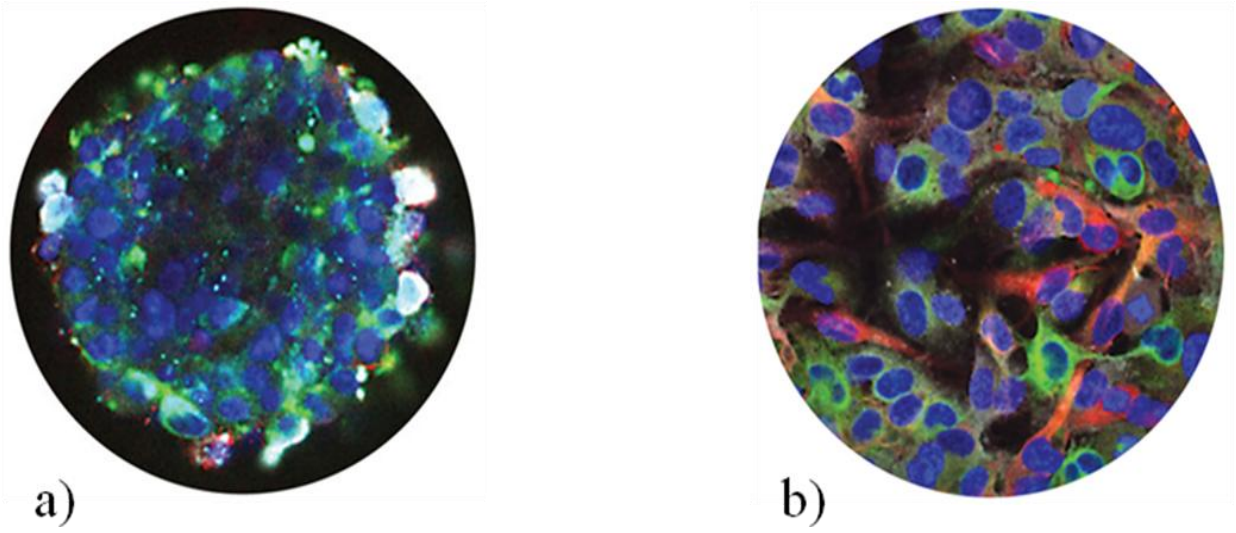

Fig 1.3: Fluorescent micrographs (red stains for GFAP+ astrocytes, whereas turquoise and green stain for oligodendrocyte O4 and β-tubulin markers respectively) showing high-grade glioma cells growing as: a) spheres in culture (more aggressive behavior), b) monolayer in culture (better differentiated tumors). Photos from: North Central Cancer Treatment Group at Mayo Clinic (USA)

Firstly isolated, characterized and described by Lawrence F. Eng in 1969, GFAP is a type III IF protein that maps in humans to 17q21 (Bongcam-Rudloff et al, 1991; Eng et al, 2000). Being closely related to its non-epithelial family members, such as vimentin, desmin, and peripherin,

which are all involved in the structure and function of the cell's cytoskeleton, GFAP is thought to help maintaining astrocytes' mechanical strength and shape.

Noteworthy, GFAP is necessary for many critical roles in the central nervous system (CNS): it is pivotal during mitosis, as confirmed by the increase in the amount of phosphorylated GFAP during this phase of cellular life, it plays a role in astrocyte-neuron interactions as well as cell-cell communication, and has been linked to multiple degenerative processes including abnormal myelination, white matter structure deterioration, and functional/structural impairment of the blood–brain barrier (Liedtke et al, 1996).

Finally, GFAP is a potentially informative plasma biomarker for gliomas being detected in plasma samples of every patient with high-grade glioma (Husain et al, 2012). Because of its role in cell's differentiation, only well differentiated cells retain the ability to express it (see Fig 1.3), while the most aggressive ones lose this typical feature at a certain point in their dedifferentiation process (Singh et al, 2003).

Beside GFAP, other proteins of interest are now being advocated for early diagnosis or monitoring of glioma. To this regard collection or panels of such proteins as opposed to a single biomarker will be necessary for a reliable diagnostic improvement in terms of accuracy (Rasooly et al, 2006). In general, to realize the full potential of clinical biomarkers, new bioanalytical technologies are being developed with the aim to achieve an accurate detection at low volumes (till to pg/ml) of panels of biomarkers (Kingsmore et al, 2006)

1.4 From Micro- to Nanobiosensors for protein recognition: state of the art

A biosensor is a device that combines a biological component with a physicochemical detector used for the recognition of an analyte at a micro- or nanoscale. An indispensable requirement for any biosensor is an excellent specificity and sensitivity for biomarkers detection, the former can be defined as the ability of the assay to rule out a condition when a specific biomarker is absent, while the latter is defined as the ability of the assay to identify a condition when it is present (Rusling et al, 2010). Those clinical specificity and sensitivity parameters are closely linked to the method used for measurements, and need to be high (>90%) to avoid false positive or false negative results (Moncada et al, 2008).

The sensitive biological elements of biosensor, generally represented by biologically derived materials or biomimetic components (i.e. tissue, microorganisms, enzymes, antibodies, nucleic

acids, etc.), interact throughout specific binding to, or recognition of, the analyte under study. The detector element or transducer, which works in a physicochemical way (i.e. optical, piezoelectric, electrochemical, etc.), transform the signal resulting from the interaction of the analyte with the biological element into another signal that can be more easily measured and quantified.

Detection elements play a key role in analyte recognition in biosensors: therefore detection elements with high analyte specificity and binding strength are required. While antibodies (Abs) have been increasingly used as detection elements in biosensors, some key challenges remain: their immobilization on the biosensor surface and the optimal method for identifying the antigen-antibody interaction.

According to the array-based optical, mass-detection or radio-labeled read out, micro and nanobiosensors can be classified as follows:

1.4 a) Optical read-out

Optical biosensors account for the most known and widespread devices and protocols for detection of bioanalytes, including enzyme-linked immunosorbent assay (ELISA), which is particularly useful for a plate-based detection and quantification of substances such as peptides, proteins, antibodies and hormones.

In an ELISA assay, an antigen must be immobilized to a solid surface and then complexed with an antibody that is linked to an enzyme; the detection is accomplished by assessing the conjugated enzyme activity via incubation with a substrate to produce a measureable product, which generally is a detectable fluorescence signal. Therefore the most crucial element of the detection strategy is a highly specific antibody-antigen interaction.

ELISAs are typically performed in polystyrene plates, which will passively bind Abs and proteins; having the reactants of the ELISA immobilized to the microplate surface makes it easy to separate bound from nonbound material during the assay. This ability to wash away nonspecifically bound materials makes the ELISA a powerful tool for measuring specific analytes within a crude preparation.

ELISAs can be performed with a number of modifications to the basic procedure (see Fig 1.4): the key step, immobilization of the antigen of interest, can be accomplished by direct adsorption to the assay plate or indirectly, via a capture antibody that has been attached to the plate. The antigen is then detected either directly (labeled primary antibody) or indirectly (labeled secondary antibody).

The most powerful ELISA assay format is the sandwich assay. This type of capture assay is called a “sandwich” assay because the analyte to be measured is bound between two primary Abs: the capture antibody and the detection antibody.

The sandwich format is often the preferred one because it is more robust and equally sensitive then direct or indirect assays.

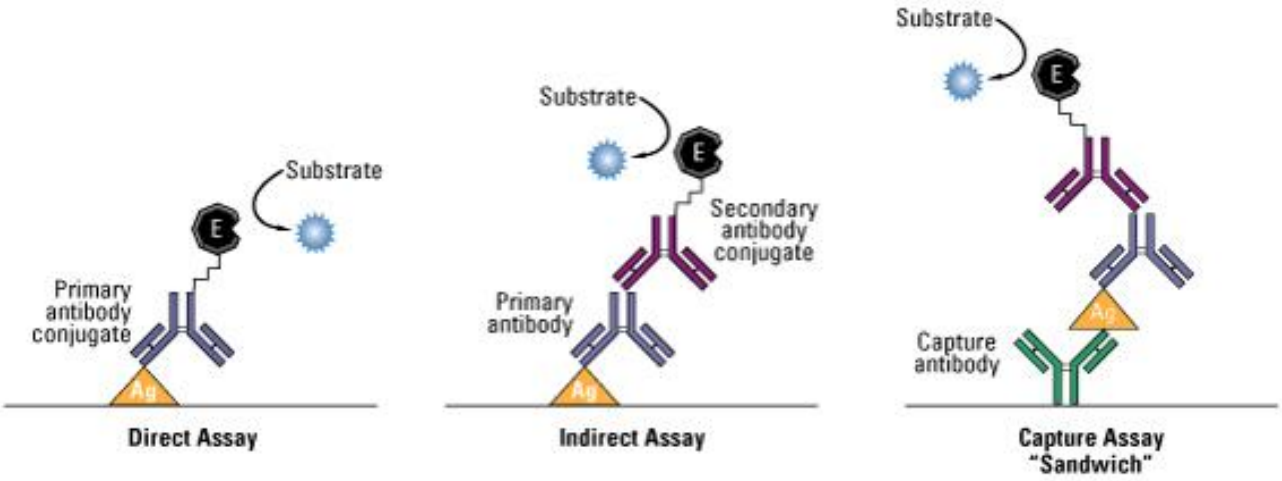

Fig 1.4: Schematic representation of the most common ELISA formats.
Drawing from: Thermo Fisher Scientific Inc

ELISA is nearly always performed using 96-well or 384-well polystyrene plates and samples in solution (i.e., biological fluids, culture media or cell lysates); however, other variants of ELISA exist:

- ELISPOT (enzyme-linked immunospot assay) refers to ELISA-like capture and measurement of proteins secreted by cells that are plated in polyvinylidene difluoride (PVDF)-membrane-backed microplate wells. It is a "sandwich" assay in which the proteins are captured locally as they are secreted by the plated cells, and detection is with a precipitating substrate. ELISPOT is like a Western blot in that the result is spots on a membrane surface (Czerkinsky et al, 1983)
- In-cell ELISA is performed with cells that are plated and cultured overnight in standard microplates. After the cultured cells are fixed, they undergo a permeabilization and blocking processes, and finally target proteins are detected with Abs. This is an indirect assay, not a sandwich assay. The secondary Abs are either fluorescent, for direct measurement by a fluorescent plate reader or a microscope; or enzyme-conjugated, for detection with a soluble substrate using a plate reader.

1.4b) Radio-labeled read-out

The measurement of radiolabels by scintillation counting has long been one of the most reliable methods for accurate, quantitative measurement in biochemical experiments (Lees et al, 1999).

Today it has been supplanted by the ELISA method, where as previously said the antigen-antibody reaction is measured using colorimetric instead of radioactive signals; however, because of their robustness, consistent results and relatively low price per test, radio-ladeled read-out methods are again becoming popular (Godovac-Zimmermann et al, 2005).

The concepts of radio-labeled read-out have been employed in the context of proteomics, where they offered gains in absolute sensitivity and dynamic range: for instance multi-photon detection methodology, proposed as a tool to routinely and quantitatively detect radioactive labels on two-dimensional gels, has several characteristics that are advantageous for functional protein detection (Kleineret al, 2008):

- First of all, by using single particle detectors, the sensitivity for detection of radiolabels can be improved dramatically;
- Secondly, because single particle detectors can differentiate the particle energies produced by different decay processes, it is possible to choose combinations of radioisotopes that can be detected and quantified individually on the same 2D gel;
- Thirdly, this technology is essentially linear over 6 to 7 orders of magnitude (i.e. it is possible to accurately quantify radiolabeled proteins over a range from at least 60 zeptomoles to 60 femtomoles).

In principle, the implementation of chemical radiolabeling methods could provide a 100-fold decrease in the amount of biological material needed for proteomics experiments, while reducing imaging times 10–100-fold, with total amounts of radioactivity far below legal limits (Kleineret et al, 2008).

Overall, the quest for ultra-high sensitivity and quantitative precision is providing new impetus to proteomics studies: both micro- and nanoarrays hold the promise of high selectivity and sensitivity, ease of use reasonable costs per assay and good possibilities for future automation. Nevertheless several drawbacks still limit the diffusion of radio-labeled read-out: the most important ones are certainly related to the special facility, precautions and licensing required: since radioactive substances are used a gamma counter is essential to measure the radiations emitted by the radionuclide, while security issues impose strict protocols for their stocking and disposal.

1.4 c) Mass-detection read-out

Mechanical interactions are fundamental to biology, in fact on one hand mechanical forces of chemical origin determine motility and adhesion on the cellular scale, and govern transport and affinity on the molecular scale; on the other biological sensing in the mechanical domain provides unique opportunities to measure forces, displacements and mass changes from cellular and subcellular processes (Arlett et al, 2011).

The advances in micro- and nanofabrication technologies have enabled the preparation of increasingly smaller mechanical transducers, so that nowadays a promising family of biosensors is represented by micro- and nanomechanical systems, which are basically cantilever-like sensors: they are particularly well matched in size with molecular interactions, and provide a basis for biological probes with single-molecule sensitivity, indeed (Yang et al, 2006; Zougagh et al, 2009). Recently, detection of mass in the zeptogram range and sensitivity in liquid to the fraction of nM concentration in real time has been demonstrated (von Muhlen et al, 2010).

Despite biosensors based on nanomechanical systems have gained considerable relevance in the last decade, several theoretical and experimental studies, reporting the influence of the mass transport on antibody biosensors as a function of analyte concentration and incubation time, concluded that pushing the sensitivity to the limit of single molecule detection may not bring the expected benefit to the overall performance (Nair et al, 2006; Sheehan et al, 2005).

In fact mass transport can significantly lower the practical sensitivity of a device by reducing the number of binding events (Tamayo et al, 2013). Moreover, especially at low concentration, which is typical of biomolecular experiments, the interaction between target molecules and the biosensor can play as critical a role as the chemical reaction itself in governing the binding rate (Kusnezow et al, 2006).

In the attempt to overcome these limitation Melli and colleagues developed a micromechanical sensor (see Fig 1.5) based on vertically oriented oscillating beams (or pillars) which make it possible to locate the sensitive area at the free end of the oscillators (Melli et al, 2011).

Practically, an array of such pillars (3μm x 8μm in plane, and 15μm in height) behaves as an array of isolated nanosized sensors embedded in a quasi-infinite analyte solution: while the top face of the pillars represents the nanosized active area, the pillars themselves can be operated as mass detectors. In particular these three-dimensional structures with dimensions comparable to the diffusion length of the target molecules have proved to increase the reaction speed by 3 orders of magnitude, while attaining improvement also in concentration sensitivity.

Fig 1.5: Micromechanical pillars. Photo from: Melli M et al, ACS Nano 2011

1.4 d) Mechanical-sensing read-out

To conclude this digression on micro- and nanobiosensors it is also useful to cite that in the last decade, the quest for protein detection in smaller volumes, along with continuous efforts to monitor specific interactions between Abs and antigens employed in an immunoassay system have led to the development of several ELISA like biosensors, including Atomic Force Microscopy (AFM) based arrays.

AFM is a very high-resolution type of scanning probe microscopy, consisting of a cantilever with a sharp tip (probe) at its end that is used to scan the specimen surface, a laser to measure any probe deflection and reflect it from the top surface of the cantilever into an array of photodiodes; the tip-sample intermolecular forces are detected, as a function of the distance between the two (Picas et al, 2012).

The AFM can be operated in a number of modes, depending on the application: basically AFM imaging may be divided into static mode (also called contact) and a variety of dynamic modes (non-contact or "tapping") where the cantilever is oscillated. The stiffness of the cantilever determines the ratio between the distance moved and the force exerted by the surface, therefore this parameter is most relevant for determining the tip-sample interaction during the majority of AFM operation modes.

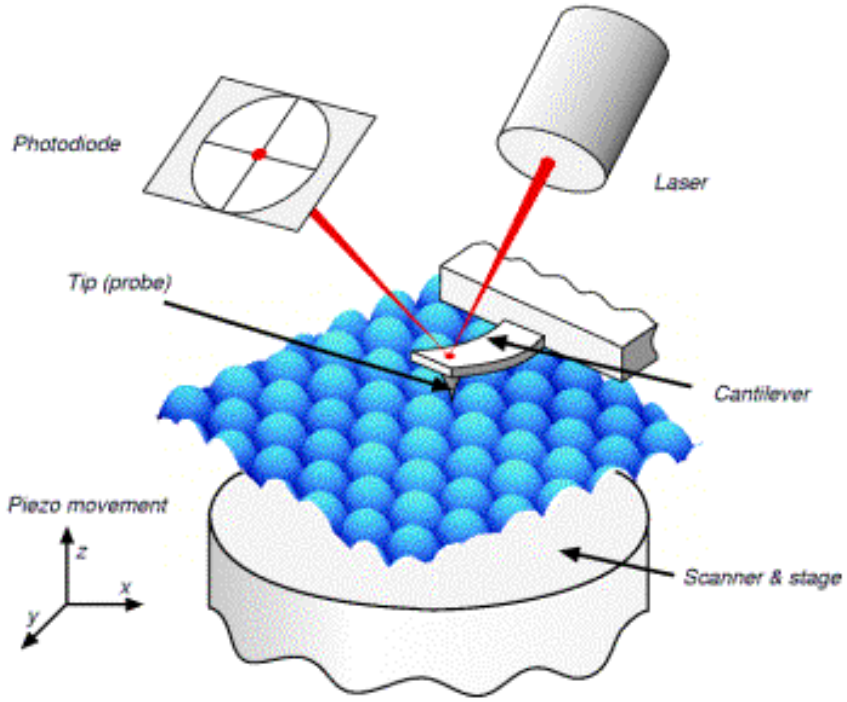

Fig 1.6: Schematic illustration of the AFM: the tip is attached to a cantilever, and is raster-scanned over a surface. The cantilever deflection due to tip-surface interactions is monitored by a photodiode sensitive to laser light reflected at the tip backside; the position of the reflected beam is kept centered in the diode through feedback-controlled z-changes in the stage.
Drawing from: Dept of Pharmaceutical Physical Chemistry, Uppsala University (Sweden)

For instance while medium stiffness cantilevers are well suited for patterning of surfaces (i.e. nanografting); on the other hand, since to obtain quality images it is critical that the AFM tip not damage the surface being scanned, softer cantilevers (< 0.04N/m) allowing to image surfaces with very low forces, are the most indicated to avoid undesirable surface modifications.

AFM is a powerful technique for investigating surfaces by visualizing their topographic characteristics: even very low number of target molecules can be reliably detected using height and/or compressibility measurements. Starting from the works of Liu and colleagues it has been consistently demonstrated that accurate height measurements of nanopatches before and after sequence specific hybridization of DNA oligomers allow for reliable, sensitive and label-free detection of hybridization itself (Liu et al, 2005; Liu et al, 2008, Mirmomtaz et al, 2008).

Moreover, AFM probes may also be functionalized: in 1997, Allen and colleagues were the first to use AFM probes functionalized with ferritin to monitoring the adhesive forces between the probe and anti-ferritin antibody-coated substrates (Allen et al, 1997).

Recently, Volkov and colleagues demonstrated that a reliable reading of the immunosignal (a suggested dimensionless combination of brush length and grafting density) can be obtained from

an area as small as ~3μm^2: approximately 4 million times smaller compared to typical ELISA sensors (Volkov et al, 2010). Intriguingly, they found that AFM could reliably distinguish between having the immunosignal from either antibody and from both Abs together: attaining a new detection limit that was impossible to obtain by using standard optical methods.

1.5 Micro- and Nanofabrication strategies: overview

The basic concept of several techniques for fabrication and biopatterning of surfaces at the micro- and nanometer scale, including photolithography, microcontact printing, dip pen nanolithography, AFM nanografting will be described in the following pages. To conclude, special attention will be drawn to the DNA-directed immobilization (DDI), a bottom up biofunctionalization technique particularly suitable for a high-sensitivity determination of panels of biomarkers.

1.5 a) Photolithography

Photolithography is a very cost-effective process used in microfabrication to pattern thin films: in other words it allows to transfer a geometric pattern from a photomask to a light-sensitive chemical photoresist on the substrate. A series of chemical treatments is then used to enable deposition of a new material in the desired pattern upon the material underneath the photoresist.

Photolithography enables scientists to create extremely small patterns (down to a few tens of nm in size), while maintaining exact control over the shape and size of the objects created.

Photolithography requires a clean room and combines several steps in sequence (see Fig 1.7) for the microfabrication of masters and the subsequent process of replica molding of the masters in poly-dimethylsiloxane (PDMS).

- Organic or inorganic contaminations are firstly removed by wet chemical treatment (generally with solutions containing hydrogen peroxide) and wafers are used as substrates to fabricate the master molds.
- The wafers are then heated to a temperature sufficient to drive off any moisture that may be present on their surface, and covered with the photoresist by spin coating. Immediately after spinning, the wafers must be baked to drive off excess of photoresist solvent, and afterwards exposed to a UV dose of 375 to 240mJ/cm^2 (depending on the thickness of the SU 8) on a contact aligner.

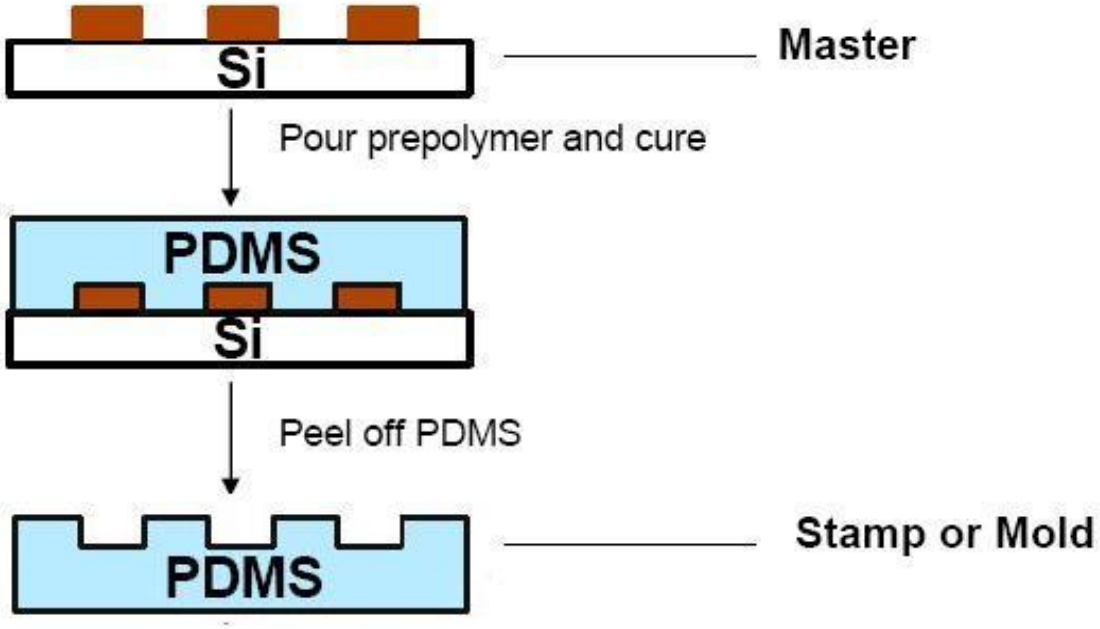

Fig 1.7: Microfabrication process: PDMS prepolymer is poured onto a photolithographically patterned master; after curing PDMS is peeled away and microwells are ready to be functionalized for deposition of living cells. Drawing adapted from: Dept Biomedical Engineering, UCIrvive (USA)

- The masters are further treated to render the exposed surface very inert, which facilitate the release of the PDMS mold after curing.
- The PDMS is ready to be degassed and poured onto the master, then degassed again and cured in a 65° oven for 1 to 16h. Once cured, the PDMS is manually peeled off the master, and the resulting structure (i.e. the microwells) are ready to be functionalized.

1.5 b) Microcontact Printing

For a while photografting of proteins was obtained from classical photolithographic techniques; in 1993 a novel approach, called microcontact printing, was introduced by Whitesides and colleagues for patterning SAM of alkanethiols onto gold substrates (Kumar et al, 1993; López et al 1993).

To date, microcontact printing is widely used for generating micropatterns of nanomaterials such as organic molecules and biomolecules over large surface areas (>cm2). In the microcontact printing process, a microstructured elastomer stamp is coated with a solution of a nanomaterial and applied to a substrate of choice, then after a given period of time in conformal contact (generally

overnight), the stamp is removed leaving a replica of the stamp pattern on the substrate surface (see Fig 1.8).

The elastomer stamps are made typically from PDMS by curing liquid prepolymers of PDMS on a lithographically prepared master. The elastomeric properties of stamps made of PDMS ensure conformal contact (intimate contact) with various substrates.

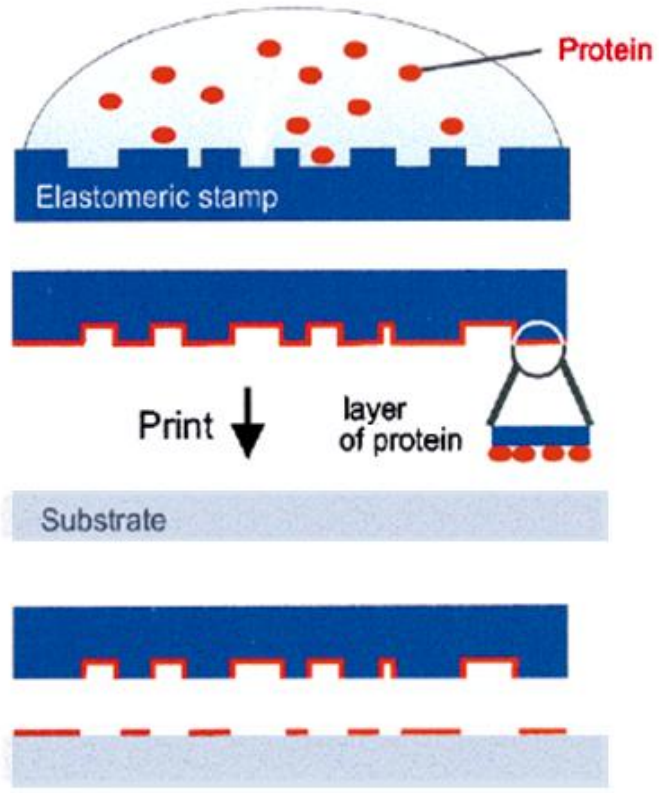

Fig 1.8: Scheme of microcontact printing: a conventionally fabricated PDMS stamp serves as the vehicle to transfer the ink of choice, in this case proteins, upon brief contact; then the transfer of those proteins occurs only at the sites of conformal contact between stamp and substrate.

Drawing from: Bernard A et al, Adv Mater 2000

As the stamps can be structured with almost any pattern, conformal contact can be achieved in many different geometrically conformed ways.

Moreover, since this technique is carried out under room temperature, different biomolecules may directly be transferred in a controlled way onto a variety of substrates while retaining their biological activity. However the deposition of liquid samples followed by drying could be very complex, leading to ill-defined patterns, protein aggregation and loss of biological activity.

Noteworthy, this problem has recently been overcame by extending these concepts to the nanoscale dimensions in a process referred to as nanocontact printing, so that, features as small as 40nm can now be fabricated by this way (Li et al, 2003). Nanocontact printing has been achieved by decreasing the feature sizes in the PDMS stamp and diluting the nanomaterial inks, utilising special variants of PDMS stamps or employing new polymeric material stamps. Another important factor on obtaining high resolution prints at the 100nm level relates with the ink utilised, to this regard biomolecules are attractive nanocontact printing inks since their high molecular weight prevents diffusion during the printing step, resulting in high-resolution features.

As opposed to the parallel conventional photolithographic process, nanocontact printing is not diffraction limited and makes possible to pattern surfaces with molecular sized features. A significant advantage of nanocontact printing lithography compared to serial techniques such as dip-pen nanolithography (DPN) is that large areas can be nanopatterned rapidly.

Nevertheless, multicomponent biomolecule nanopatterning is still very problematic with this technology due to the practical difficulties in accurately aligning multiple flexible stamps over a large area while maintaining a nanoscale resolution, and thus further development is required to solve this problem.

1.5 c) Dip Pen Nanolithography

While studying a process through which molecules could be transferred to a wide variety of surfaces to create stable chemically-adsorbed monolayers in a high resolution lithographic process, Mirkin and colleagues termed DPN a scanning probe lithography technique where an AFM tip was used to transfer alkane thiolates to a gold surface (Mirkin et al, 1996; Piner et al, 1999).

DPN allows surface patterning on scales of under 100nm, and is the nanotechnology analog of the dip pen (also called the quill pen), where the tip of an AFM cantilever acts as a "pen," which is coated with a chemical compound or mixture acting as an "ink," and put in contact with a substrate, the "paper." DPN enables direct deposition of nanoscale materials onto a substrate in a flexible manner.

Recent advances have demonstrated massively parallel patterning using two-dimensional arrays of 55,000 tips. Applications of this technology currently range through chemistry, materials science, and the life sciences, and include fabrication of ultra high density biological nanoarrays (Chai et al, 2011).

1.5 d) AFM Nanografting

Nanopatterning of surfaces for biomedical applications has been of growing interest in recent years, from both scientific and technological points of view: indeed diverse biological and medical applications can be envisioned such as biochips and biosensors.

To this regard nanotechnology not only offers the reward of smaller dimensions with more reaction sites, but also smaller test sample volumes and potentially higher sensitivity and throughput screening for molecular diagnostics.

Beside its uses as imaging tool, the AFM can also be exploited for a fine nanopatterning of surfaces: if compared to other methods of nanofabrication, nanografting allows more precise control over the size and geometry of patterned features and their location on the surface. The technique of nanografting is usually used on self assembled monolayers (SAMs) and is achieved in the presence of a second replacement surfactant molecule with a greater affinity for the surface, or concentration in the grafting solution than the molecule being removed by the AFM tip (see Fig 1.9). Therefore, once the pre-formed SAM is removed from the desired area by the AFM tip, it will be replaced with a second surfactant to form a new SAM in the patterned area.

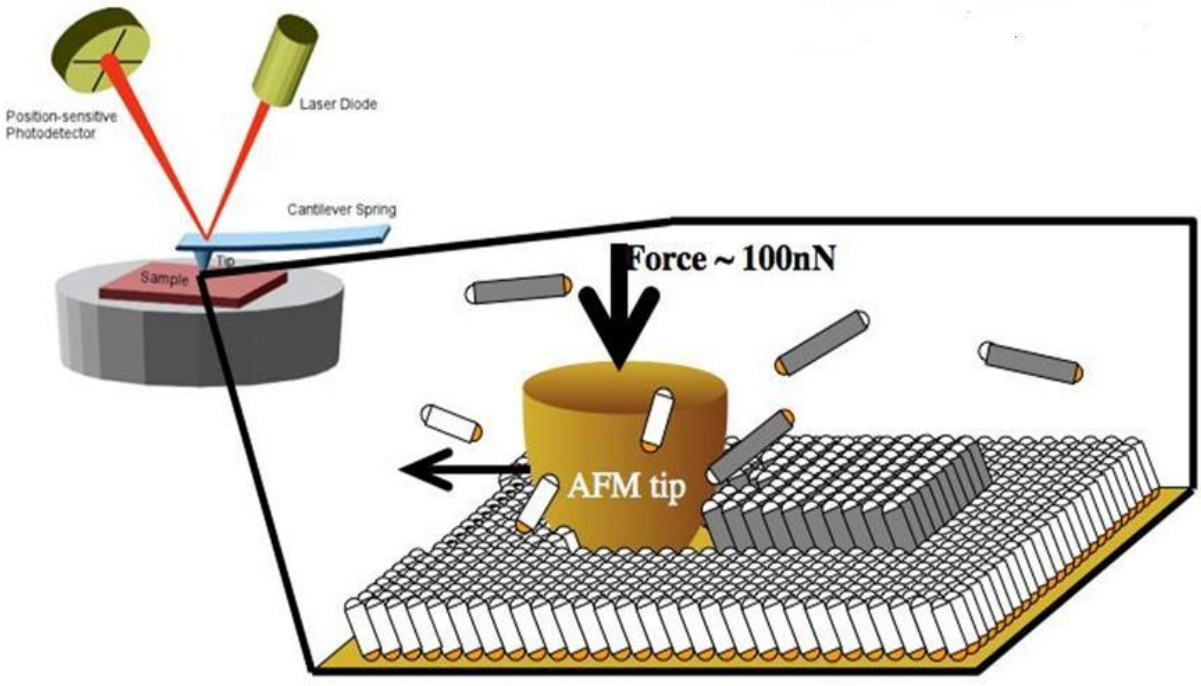

Fig 1.9: Representation of AFM based nanografting: once the pre-formed SAM is removed from the desired area by the AFM tip, it will be replaced with a second surfactant to form a new SAM in the patterned area. Drawing from: Xu S et al, Langmuir 1997

Noteworthy, some criteria need to be met: the SAM must be readily removable with the force applied by the AFM tip, but more importantly, the second surfactant must form the new SAM rapidly. It is for these reasons that thiol SAMs on gold are usually the system of choice for nanografting experiments, due to the way in which thiols rapidly form homogenous monolayers on exposed gold surfaces. This strategy may be used for the production of nanometer-sized protein patterns on gold surfaces by exploiting the affinity of biomolecules towards different SAMs (Liang et al, 2012).

AFM based lithography methods are attractive nano-arraying techniques and have shown many potentialities in generating arrays with significantly reduced amount of capture materials, such as DNA, peptides and Abs. Further, these methods exploit the AFM tip (radius of curvature below 10nm) to selectively pattern complex structures on the surface and can offer high sensitivity and resolution.

By varying fabrication parameters, as the number of scanning lines at high tip load set in a given surface area, the speed of the AFM tip, the concentration of molecules in solution, etc the numbers of molecules released to the surface can be appropriately tuned. In the pioneering work of Mirmomtaz, our group showed that by nanografting DNA nanostructures patches of predetermined different height could be reproducibly created (Mirmomtaz et al, 2008).

Moreover recent investigations demonstrated the correlation between patch height and DNA molecules surface density in the range of 10^{12} - $3x10^{13}$ mol cm^{-2} (Castronovo et al, 2011; Bosco et al, 2012)

The great advantage of AFM patterning is that the same technique may be used for both patterning and imaging a SAM as several physical and mechanical properties can be measured all at once.

The topographic height of the patches is used to infer any change at any step of the nanoassay, and, concertedly with the measurement of the roughness, within and outside the patch, constitute a unique method not only to quantify the bio-recognition events, but also to rule out the presence of unspecific molecular adsorption.

Other advantages of this technique include (Bano et al, 2009; Sanavio et al, 2010):

- the possible identification of molecular orientation by measuring the molecular height with high precision (order of Angstroms) with respect to a supporting substrate,
- the well defined patterning of homogeneously oriented molecules,
- the possibility of printing multiple features in array format, where different molecules are placed selectively at different sites.

1.5 e) DNA-Directed Immobilization

Diagnostic immunoassays and DNA sensing are driving efforts to miniaturize biological assays and to conduct them in parallel; specifically, DNA-based arrays are becoming the leading technology for high integration and miniaturization of bioassays (Schena et al, 1995; Bernard et al, 2000).

The use of DNA microarrays technology for proteomics known as DDI was introduced in 1994 by Niemayer and colleagues showing that covalent DNA-streptavidin conjugates could be utilized for the reversible and site-selective immobilization of various biotinylated enzymes and antibodies (Niemayer et al, 1994).

Their pioneering experiments demonstrated that enzymes, such as biotinylated alkaline phosphatase, beta-galactosidase, or horseradish peroxidase, as well as antibodies, such as biotinylated anti-mouse or anti-rabbit immunoglobulins, could be coupled to the DNA-streptavidin adapters by simple, two-component incubation, and that the resulting preconjugates could be exploited to hybridize complementary oligonucleotides by surface-bound (Niemayer et al, 1999; Niemayer, 2002; Niemayer, 2012).

DDI proceeds with a higher immobilization efficiency than conventional immobilization techniques because of the reversible formation of the rigid, double-stranded DNA spacer between the surface and the proteins.

The simultaneous immobilization of different compounds using microstructured oligonucleotide arrays as immobilization matrices demonstrates that DDI proceeds with site selectivity due to the unique specificity of Watson-Crick base pairing; moreover, it allows for a reversible functionalization of the sensor surfaces with the proteins of interest.

Since DDI technologies and DNA nanoconstruction essentially depend on similar pre-requisites, which in particular are: large and uniform hybridization efficiencies, combined with low nonspecific cross-reactivity between individual sequences, this microarray approach has emerged along the last years as a promising tool for chip-based immunoassay meant to multiplex antigen detection.

In fact, it is well known that the self-assembly of semi-synthetic DNA-protein conjugates in so called nano-assembled monolayers (NAMs) makes it easy to generate unlimited reproducible, configurable nanoarrays exploiting precise and reliably proteins/Abs detection methods (see Fig 1.10).

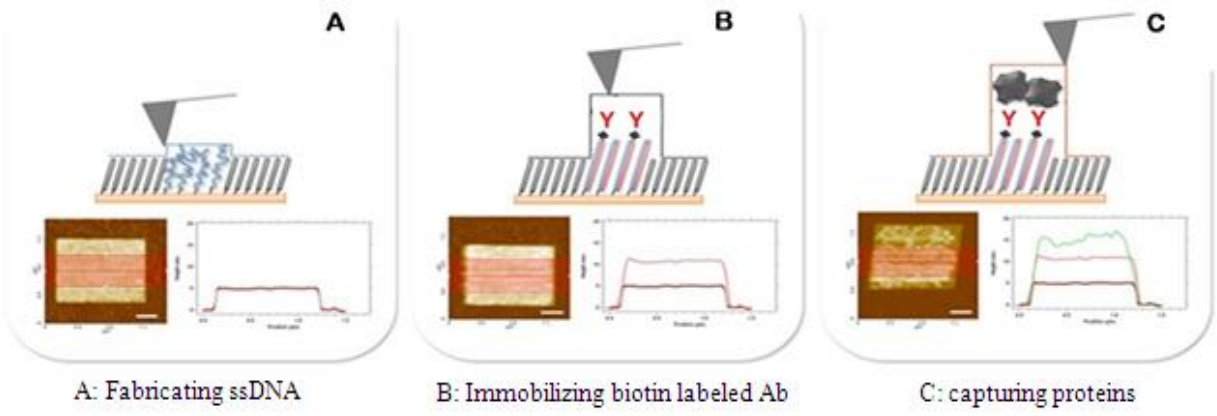

Fig 1.10: Schematic representation of the three steps involved in DDI: A) ssDNA grafting, B) immobilization of the antibody of interest by hybridization with the complementary strand of DNA, C) immobilization of the protein of interest. Drawing adapted from Sanavio B et al, ACS Nano 2010

DDI allows for highly economical use of antibody materials (at least 100-fold lower than the amount needed for preparing an array by direct spotting), therefore taking into account the greater versatility and convenience of handling of the self-assembly approach, DDI proved to be an advantageous alternative to conventional techniques for generating versatile and robust protein arrays.

The DDI strategy bears the potential for relatively rapid high sensitivity determination of limited panels of biomarkers with good precision and accuracy.

Despite its potential to revolutionize protein diagnostics, the major problems in the fabrication of such antibody arrays concern the initial efforts required to reproduce homogeneously the attachment of the antibody on the DNA substrate.

To this regard, protein recognition could eventually be carried out in a single step by directly grafting the double strand DNA already bound with the antibody of interest onto the SAM, such advancement could significantly reduce both the procedural steps needed and relative handling time, as well as the costs of analysis in the near future.

1.6 Aim of the research

In this research we have chosen to exploit all the potentialities of microfrabrication, nanofunctionalization and imaging described in the previous pages to develop a new diagnostic tool (see Fig 1.11).

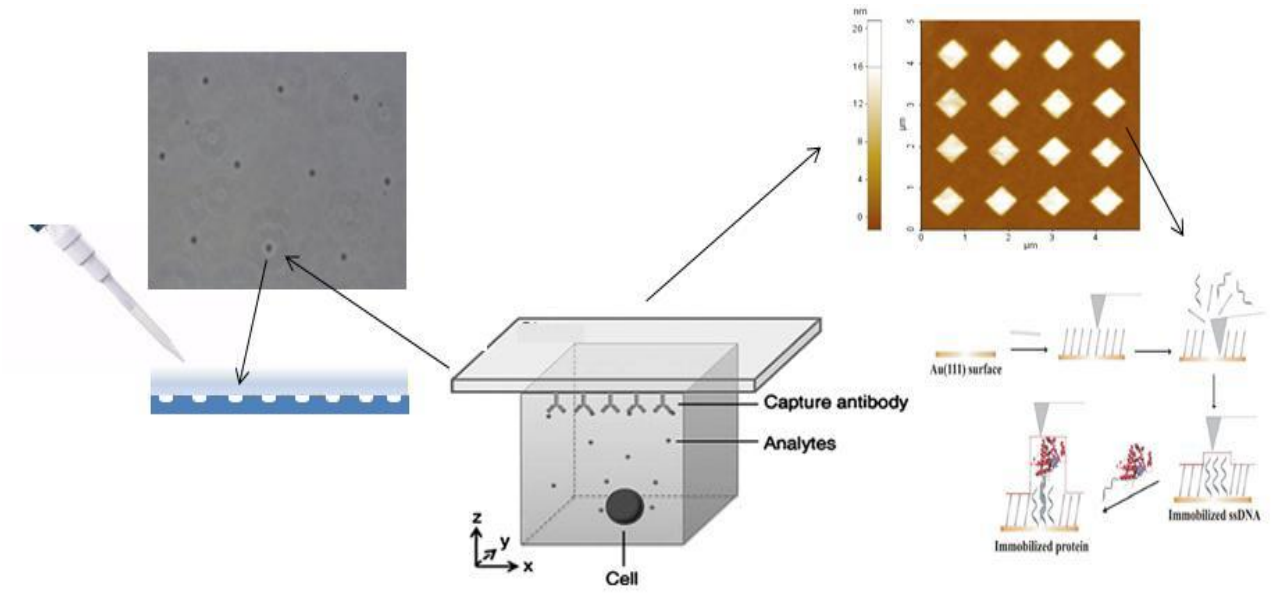

Fig 1.11: Schematic representation of the device.
Drawings adapted from Bano F et al, NanoLett 2009

In fact, to fulfil the abovementioned goal of enabling a precise, high throughput and low cost *in vitro* analysis of tumor cells' lysate, or, *in vivo* studies, also of their secretome, down to the single cells level, we developed a device consisting in micro-fabricated wells capable to isolate and host living astrocytes (ideally, one cell per micro-well).

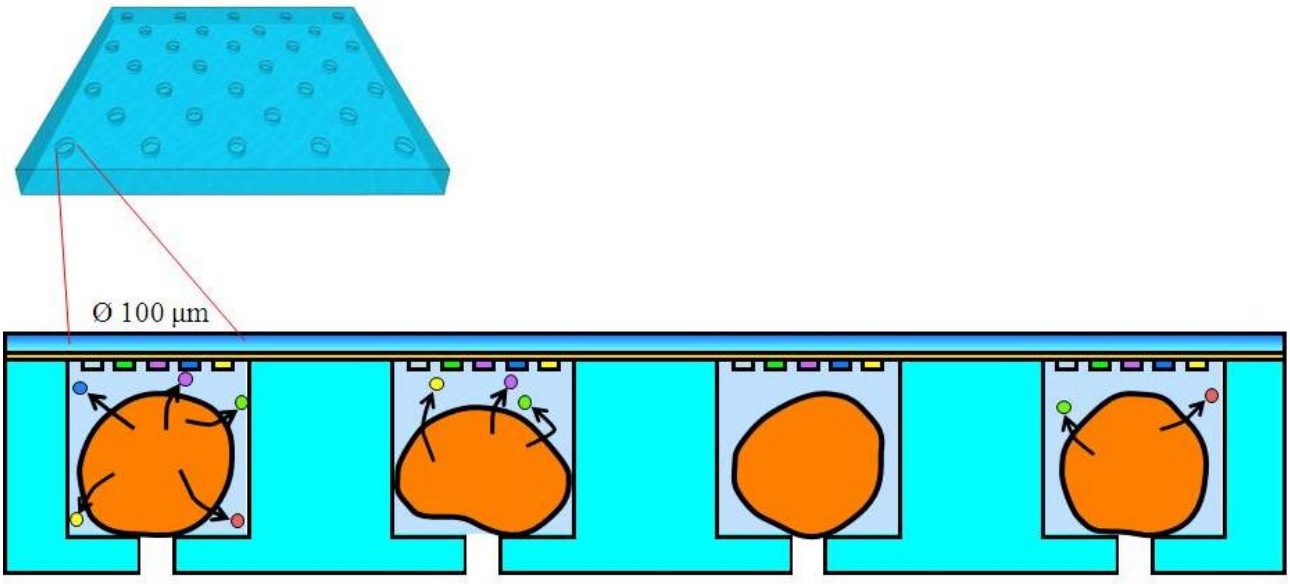

Fig 1.12: Schematic drawing of the cells immobilized in each microwell and faced to the functionalized nano-immuno arrays

Beside tailoring the processes of microfabrication to create wells suitable for hosting living cells, the utmost attention was paid to the optimization of the multiple steps required to functionalize those microwells: an indispensable pre-requisite for enabling cell adhesion, especially when dealing with eukaryotes.

Then, to create an effective biosensor, able to detect in such small volumes the presence of the proteins of interest, ideally for multiplexing assays and meant to fit within the small dimensions of this microdevice, we challenged the optimization of protocols for immobilization of antibodies onto surface tethered, spatially constrained DNA patches.

Accordingly, we prepared nanosized immuno patches specific for the recognition of GFAP on a SAM of top-terminated oligo-ethyleneglicol alkanethiol-modified (TOEG) gold surface, in order to use the solid matrix with nanopatches as the ceiling of each microwell (see Fig 1.12). Toward this path, we focused toward the sensitivity implementation of the nanobiosensor, and tried to achieve that of current benchmark assays such as ELISA.

Chapter 2:

Experimental Session

2.1 Fabrication and functionalization of microwells

Microwells were obtained from a membrane of PDMS, by spin coating and replica molding (see Fig 2.1) from a reusable master with positive pillar-like relief structure (traditional photolithography using photoresist SU8 forms).

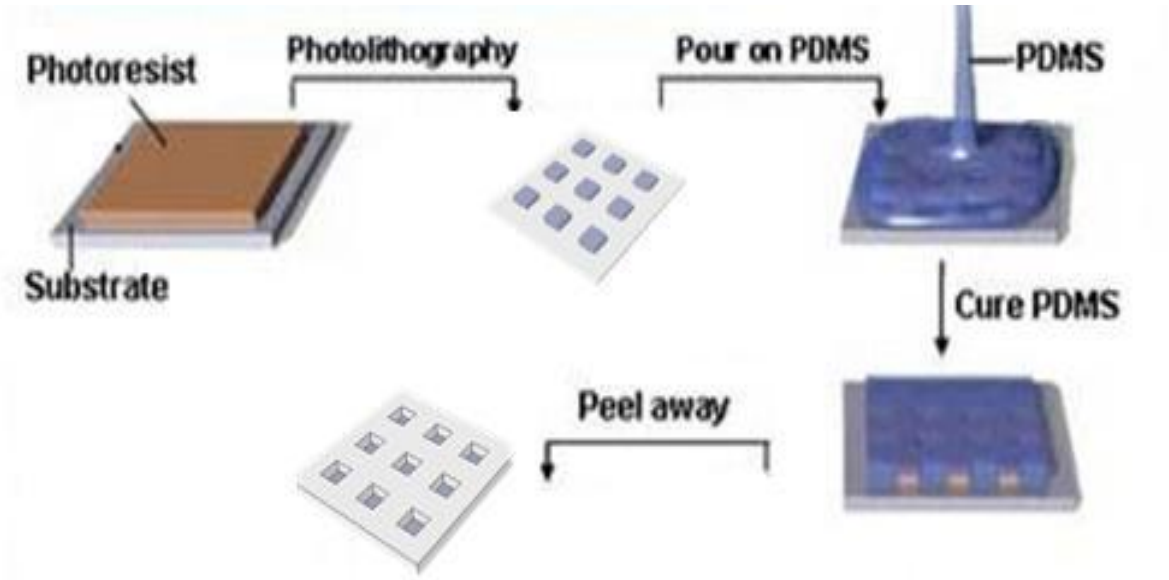

Fig 2.1: Schematic representation of microwells' fabrication

The functionalization of the floor and the walls of each well was obtained by staining the PDMS structure with a polyornithine solution (0.01% of polyornithine plus 5% of lucifer yellow) for 1h at room temperature. The excess of polyorthinine outside each microwell was removed through microcontact printing run overnight in order to clean up the PDMS within the wells.

Aiming to test the feasibility of living cells patterning within the PDMS microwells, a series of tests were conducted with different cells populations:

- On a first series of experiments the ability of prokaryotes, such as E.Coli (kindly provided by Structural Biology Lab @ Elettra), to adhere and survive with and without administration of growth medium, for at least 1h, within the microwells was tested.
- Subsequently a similar set of experiments was conducted in order to understand whether complex and fragile eukaryotes, such as hyppocampal cells (kindly provided by Spinal Biophysics Lab @ UniTS), could adhere and survive onto a PDMS surface with or without functionalization with polyornithine.

2.2 Immobilization of antibodies

For the fabrication of nanoarrays, meant to immobilize Abs specific for the protein of interest (i.e. GFAP), an approach based on AFM nanografting techniques was applied. Whilst it would be ideally desirable to directly functionalize a biosensor's surface with specifics Abs, the chemical modification to which they would be subject could affect their specificity; therefore it is still complex presently to avoid intermediate steps for Abs immobilization.

To this regard, the most common strategy is to exploit the high affinity of the streptavidin-biotin binding, working with commercially available biotinylated Abs (see Fig 2.2).

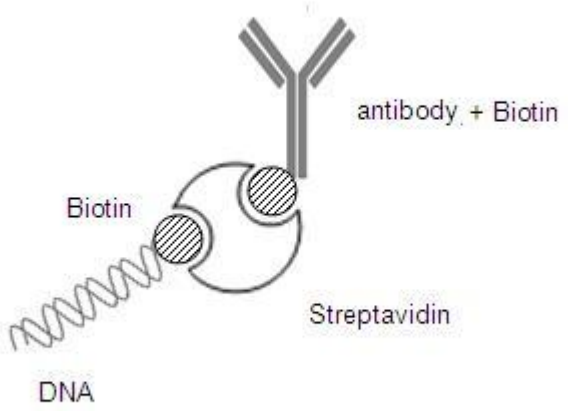

Fig 2.2: Schematic exploitation of the biotin-streptavidin affinity for specific immobilization of biotinylated Abs

Two main strategies were adopted: the first one based on fabrication of NAMs of biotin-streptavidin complexes; the others based on optimized DDI strategies.

2.2 a) Fabrication of patches of biotin terminated alkanethiol

Nanosized patches of biotin terminated alkanethiol were prepared by tip-assisted AFM nanografting inside a matrix of SAM of alkanethiol-modified gold surfaces; then streptavidin (STV) was exploited to recognize the biotin and act as an antibody binding protein for biotinylated Abs.

STV (see Fig 2.3) is a protein extensively used in molecular biology and bionanotechnology due to its extraordinarily high affinity for biotin ($K_d = 10^{-14}$ to 10^{-15}M), and the strong streptavidin-biotin complex's resistance to organic solvents, denaturants, detergents, proteolytic enzymes, and extremes of temperature or pH (Deng et al. 2012).

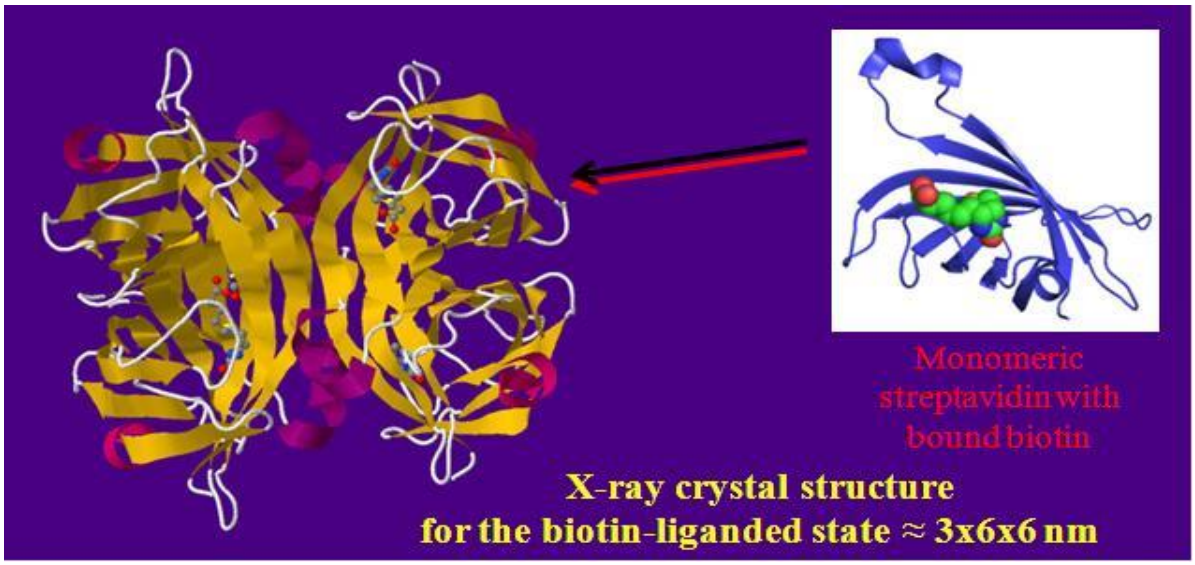

Fig 2.3: Tetrameric structure of Streptavidin. Drawing modified from Protein Data Bank

STV in its tetrameric structure presents 4 biotin binding sites, which can be exploited to both recognize the nanosized patches of biotin terminated alkanethiol, and subsequently to immobilize biotinylated monoclonal GFAP Abs on top of them (see Fig 2.4).

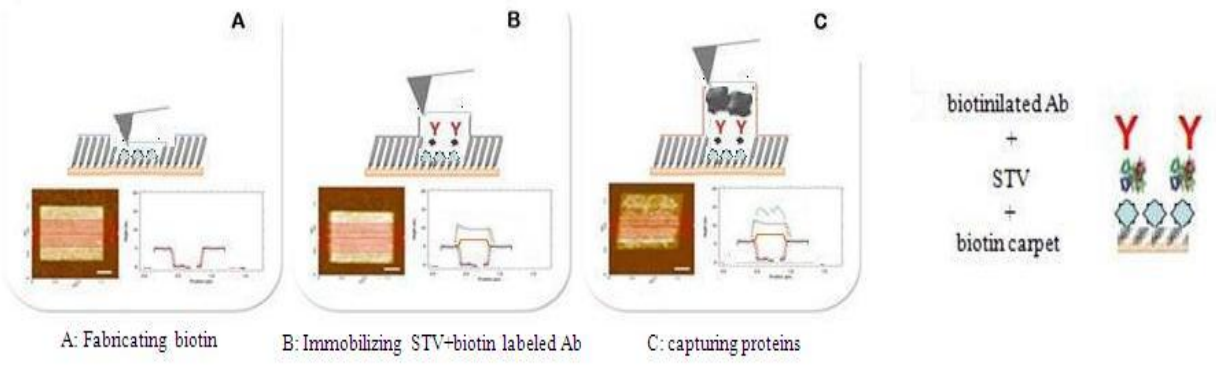

Fig 2.4: Schematic representation of the three steps involved in the fabrication of patches of biotin terminated alkanethiol: A) biotin grafting, B) hybridization of the NAM of biotin with STV and subsequent immobilization of biotinylated Abs, C) recognition of the protein of interest

A commercial AFM (Park XE-100) was utilized to obtain small patches, sized 1μm x 1μm, with an inter-patches distance of at least 2.5μm. Nanografting was conducted in a solution of biotin 5μl (50mM) in H2O plus ethanol 150μl.

The biotin patches were obtained promoting the replacement of the TOEG6 molecules with the biotin terminated alkanethiol by scanning the predetermined area of 1μm x 1μm with cantilever characterized by a stiffness of 0.6 N/m (NSC 19 MikroMasch).

During nanografting the tip was always applied at a large force (about 100nN) with a scan rate of 2000nm/s.

- This first grafting step was followed by a three series of washing with Tris(hydroxymethyl)aminomethane-Ethylene-diamine-tetraacetic acid (Tris-EDTA or TE) buffer to remove any physically adsorbed molecules before the start of the imaging session.
- The second step consisted in the incubation of the NAMs of biotin with STV by specific linking, obtained at the concentration of 500pM in Phosphate Buffered Saline (PBS) and an incubation time of 1h at room temperature.

  Even this second step was routinely followed by a thorough SAM washing (3 times with PBS) before conducting the subsequent analysis of the sample by means of AFM topographic height imaging.
- The third step consisted in the immobilization of the biotinylated monoclonal GFAP Abs onto the nanopatches (Synaptic System). A solution of 100μl of PBS containing GFAP Abs (Synaptic System) was incubated over the NAM for 1h at room temperature with a dilution ratio of 1:100.

  After a routine washing of the SAM, repeated for three times in a row with PBS the NAMs' height finally achieved was measured by the standardized AFM topographic analysis performed after each previous step.

2.2 b) Preparation of DDI of biotinylated antibodies

Multiple NAMs of thiol modified single strand DNA (ssDNA) were prepared by AFM-based nanografting inside a matrix of SAM of TOEG3 or TOEG6 surfaces.

Subsequently the preparation of multiple nanopatches, meant to act as bionanosensors, was obtained by optimizing the previously described DDI strategy (see Fig 2.5).

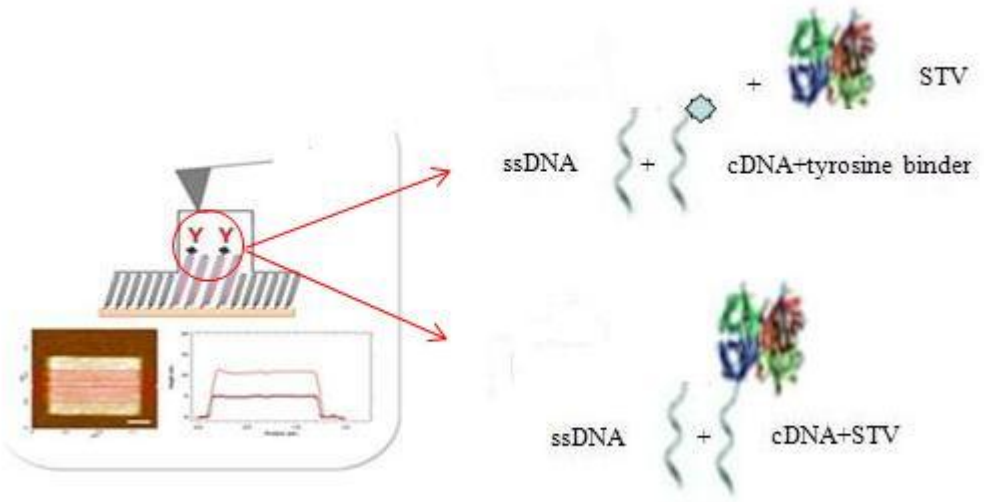

Fig 2.5: Schematic representation of the three main options to immobilize biotinylated antibodies onto DDI fabricated NAMs: the cDNA utilized to covalently bind to the ssDNA may be functionalized with a tyrosine binder-tag, necessary for the subsequent conjugation with STV, or directly with a STV-tag

The size of each patch was 1μm x 1μm, whereas the inter-patches distance chosen was 2.5 μm. Nanografting was conducted in a solution of NaCl 1M with various strands of DNA modified with a thiol linker, $(CH_2)_6SH$ (also named C6), at the 3' termination. The length of the C6 linker is about 1.2nm. C6 has the double function to link covalently the DNA to the gold surface while making the DNA molecules away from the same surface and available to hybridization with the complementary strand.

Three different strands of ssDNA were utilized:

- cF4: 5'-ctt att tta ttg tta tac gcc c-3' and its cDNA conjugated with a tyrosine binder-tag,
- cF9: 5'-ctt gat tgc cac ttt cca c-3' and its cDNA already conjugated with a STV-tag,
- cF5: 5'-ctt atc tta tga ccg gac c-3' and its cDNA already conjugated with a STV-tag.

The concentration of ssDNA utilized in each set of experiments was 5μM in TE buffer 1M NaCl; the DNA patches were obtained promoting the replacement of the TOEG molecules with the oligonucleotides by scanning an area of 1μm x 1μm with the AFM tip applying a large force (about 100nN) with a scan rate of 2000nm/s. TOEG is composed by an alkanethiol with 16 carbons plus 6 (TOEG6) or 3 (TOEG3) ethyleneglicol units, noteworthy the former is much more water soluble than the latter, making it easier for the TOEG6 to be removed during the nanografting procedure by varying the fabrication parameter (number of scanning lines in a given surface area).

- This first grafting step was followed by a three series of washing with TBS to remove any physically adsorbed molecules before the start of the imaging session.

- The second step consisted in the hybridization of the NAM of ssDNA patches with their complementary DNA strands (cDNA) by sequence specific DNA linking. The hybridization was conducted at the concentration of 500nM in TE buffer 1M NaCl with an incubation time of 1h at room temperature. Even this second step was routinely followed by a thorough SAM washing, 3 times with Tris Buffered Saline (TBS), before conducting the subsequent analysis of the sample by means of AFM topographic imaging.
- The third step consisted in the immobilization of the antibodies specific for the chosen protein of interest (always GFAP) on the top of the NAMs with or without blocking buffer solutions. Blocking buffer solutions are routinely used during antibody staining procedures (i.e. Western Blotting, direct and sandwich ELISA assays or immune-histochemistry-based protocols) to reduce background or unspecific staining; for the purposes of this experimental session two different blocking solutions were tested: Skim Milk Powder in TBS blocking buffer or BSA blocking buffer.

As in the experimental session with patches of biotin terminated alkanethiol, biotinylated monoclonal GFAP Abs (Synaptic System, GmbH) were tested onto the nanopatches. A solution of 100μl of blocking buffer containing GFAP Abs at a dilution of 1:100 was incubated over the SAM for 1h at room temperature. After a routine washing of the SAM, repeated for three times in a row with TBS (set of experiments without blocking buffer) or TBS containing 0.05% Tween 20 (TBST) plus three more times with TBS (set of experiments with blocking buffer), the NAMs' height afterward achieved was measured by AFM topographic analysis to confirm the immobilization of the GFAP Abs onto the NAMs.

2.3 Immobilization of GFAP

Aiming to further characterize a protocol suitable for multiplexing analysis, the series of experiments with DDI of biotinylated Abs were the only ones finally brought to the next level of protein immobilization.

2.3 a) Immobilization of GFAP in PBS

To avoid risks of unspecific bindings, the immobilization of GFAP onto the NAMs was initially conducted only by incubation with recombinant GFAP (Synaptic System) at a

concentration of 40nM for 1h at room temperature in a solution of blocking buffer. The subsequent AFM imaging was performed after three washes with TBST followed by three more washes with TBS.

2.3 b) Immobilization of GFAP in multicells' lysate

The suitability of those nano-immuno arrays to selectively recognize GFAP in the cells' lysate, which contains several different proteins potentially responsible for unspecific bindings over the NAMs or over the surrounding SAM, was finally tested by incubation of the SAM in a solution of 100µl of multicells' lysate (obtained from U87 cells at different concentration of 10^5cells/cc down to 10^4cells/cc) containing GFAP at a known concentration (from 40nM). The incubation was conducted at room temperature for 1h and, after a preventive washing protocol similar to those conducted after incubation in standard conditions, the height of the NAMs was analyzed by AFM to validate the experimental session.

2.4 Signal to noise ratio and roughness analyses of the SAMs and NAMs

The three preliminary steps (grafting of ssDNA, hybridization of cDNA+STV, immobilization of GFAP Abs) needed to realize the nano-immuno arrays above described, along with the subsequent immobilization of GFAP in standard conditions and in the multicells' lysate were confirmed by topographic analysis performed with AFM.

The fabricated nanopatches were imaged after resetting the value of the perpendicular force load to the smallest possible, still detectable, value. Each imaging session was conducted using a cantilever characterized by a stiffness of 0.03 N/m (CSC 38, MikroMasch) in a 300µl solution of TE or TBS or PBS (as specified above), with the following parameters: pixel size: 256 x 256, and scan rate: 1Hz. For each step not only the relative height reached by the NAMs, but also their roughness with respect to the surrounding TOEG SAM were measured by scanning side by side the patches within the SAM at a minimum force (always lower than 0nN, and in any case as much close as possible to values of set point loss) and constant speed (1000nm/s).

The imaging parameters were appropriately chosen to avoid any misleading compression of the tip over the scanned area, thus respecting characteristics acquired by the surface after each single step. All experiments were performed at least in triplicate, and the given values and errors

correspond to the mean values and standard deviation of height obtained from at least three independent patches. The evidence of a progressive NAMs' height increase was meant to confirm their selectivity in recognizing step by step the appropriate ligand.

2.5 Benchmark tests with ELISA

Being ELISA the most standardized method for protein detection, it served as a benchmark to compare the sensitivity acquired with the above-described nano-immuno array and a diagnostic tool daily used in the clinical practice.

Microtiter plates were coated with 200ng of GFAP anti-mouse IgG (Synaptic System) in 0.1 M sodium carbonate (pH 9.6) overnight at 4°C and were blocked with 3% Bovine Serum Albumine (BSA) (Sigma) in Phosphate Buffered Saline containing 0.05% Tween 20 (PBST) for 12 hours. After three washes with PBST, plates were transferred at room temperature and incubated with 100µl cells' lysates and different concentrations of GFAP protein (Synaptic System) diluted in 100µl blocking solution for 2h.

Plates were washed three times with PBST and incubated for 1h with a 1:1000 dilution of biotinylated GFAP Abs. This was followed by three washes with PBST, and an incubation of 1h with the HorseRadish Peroxidase (HRP)-conjugated Streptavidin (Millipore), in a 1:5000 dilution in blocking buffer.

Finally, plates were washed three times with PBST and developed with TMB reagent (Sigma) for 5 min before the reaction was stopped by the addition of 1M H_2SO_4. Absorbance at 450nm was measured in a plate reader (Titertek Multiskan MCC/340).

Chapter 3:

Results

Acknowledgements:

- *Luca Ianeselli for his help in the fabrication of PDMS microwells*
- *Stefania Corvaglia for her pivotal role in the functionalization of PDMS microwells*
- *Dr Alessandro Bosco for invaluable contribution with the optimization of the DDI strategy*
- *Dr Anita Palma for having run the benchmark tests with ELISA*

3.1 Patterning of living cells

The fabrication and functionalization of microwells was operationally straightforward: in fact it requires no special equipment but a clean room, and the latest step for PDMS curing and peeling can be carried out in a conventional laboratory on an inexpensive optically transparent polymeric support (see Fig 3.1).

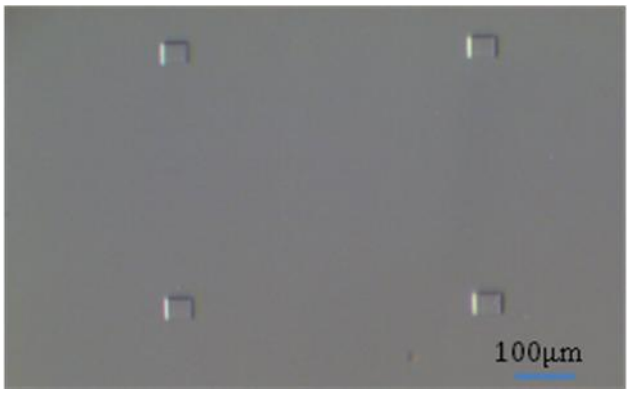

Fig 3.1: PDMS microwells

The main advantage of the PDMS substrates is that they theoretically allow to pattern any cell within microwells of the desired diameters, in order to confirm this assumption we initially tested them trying to pattern prokaryotes with microfabricated wells of very small dimensions: 10µm in diameter and 1µm in height (see Fig 3.2).

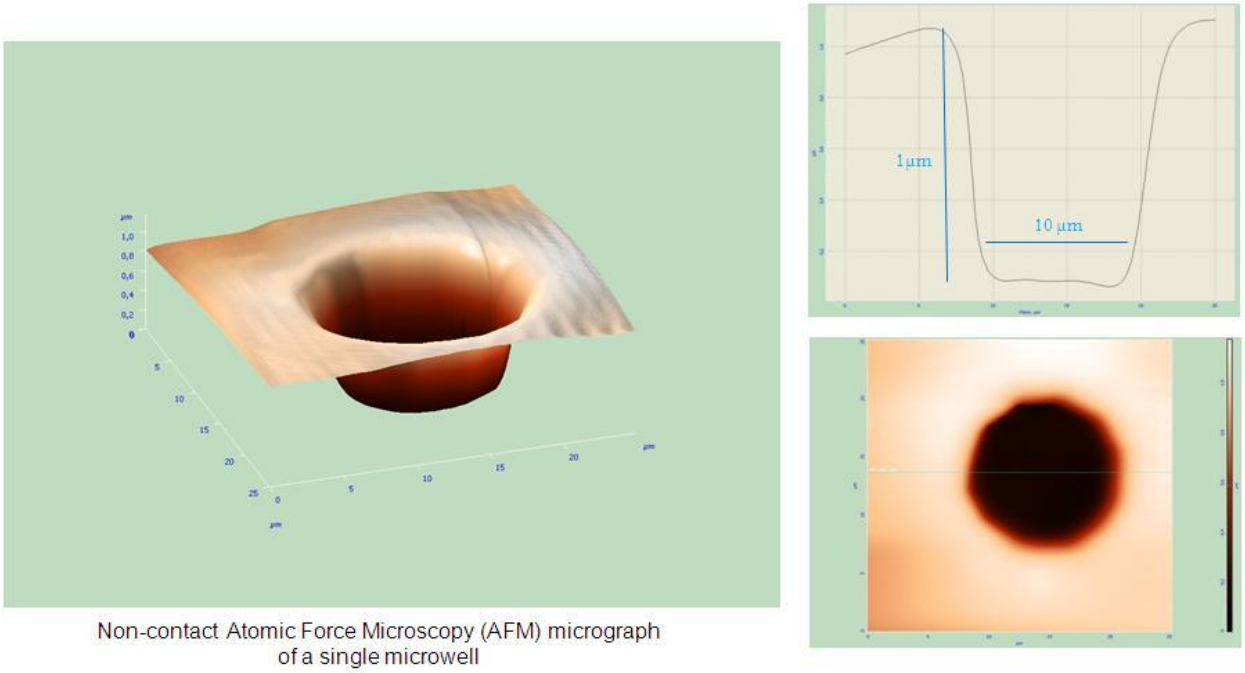

Fig 3.2: 3-D imaging of PDMS-molding microwells fabricated at IOM INFM @ TASC, Trieste

3.1 a) Tests with Prokaryotes

This set of experiments, carried out with E.Coli (see Fig 3.3), confirmed that those prokaryotes are able to adhere and survive with or without administration of growth medium, for at least 1h even within non-functionalized PDMS microwells (see Fig 3.4).

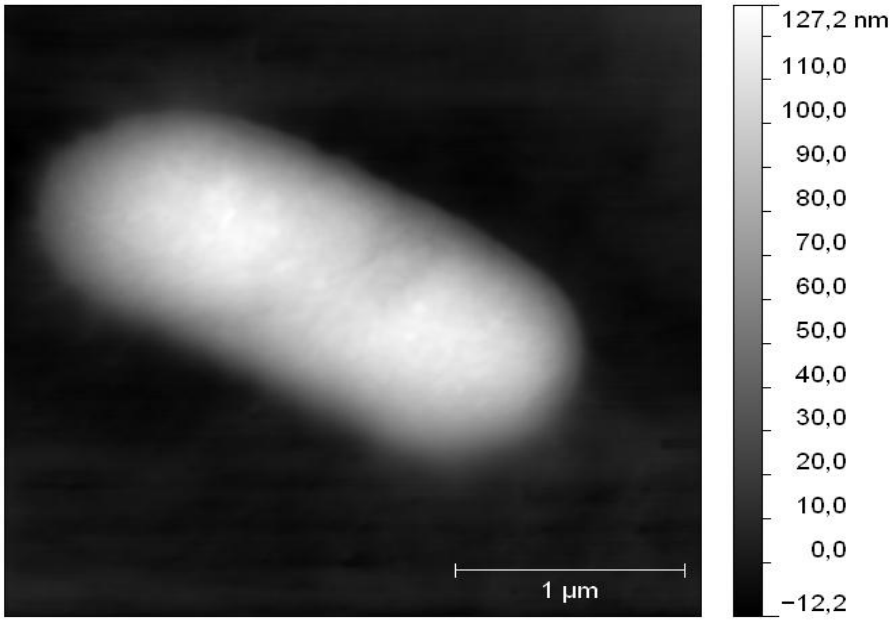

Fig 3.3: Non-contact AFM micrograph in air of E.Coli deposited onto a mica surface

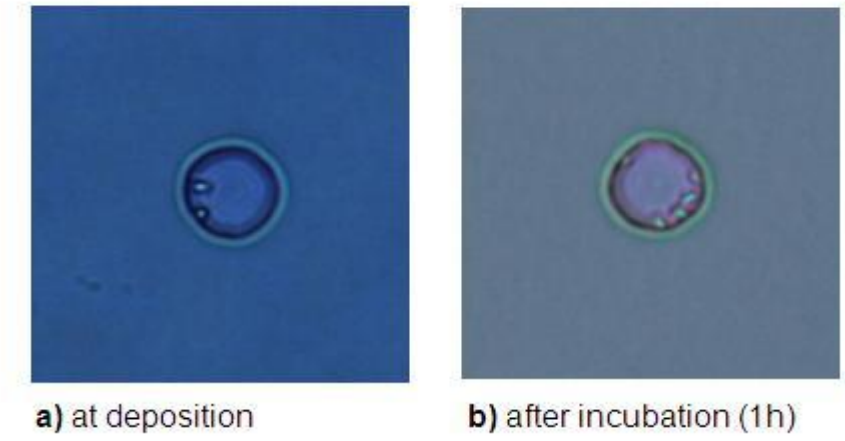

Fig 3.4: Inverted optical microscope image showing adhesion, survival and replication of E.Coli even within non-functionalized microwells

Although not operationally deemed for the prototyping of the device tested in this project, those high informative results open the way to further researches aimed at patterning living E.Coli. Noteworthy those bacteria are commonly utilized for several bioengineering purposes, therefore an

assessment of genetically modified strains of E.Coli within similar devices, appropriately created for their patterning and proteomic analysis, could be easily conducted in the near future.

3.1 b) Tests with Eukaryotes

Eukaryotic cells are typically much larger than those of prokaryotes: they have a variety of internal membranes and structures, called organelles, and a cytoskeleton composed of microtubules, microfilaments, and intermediate filaments, which play an important role in defining the cell's organization and shape. According to the final purposes of astrocytes' analysis, PDMS microwells were finally fabricated with appropriate dimensions of 100µm in diameter x 100µm in height.

Analyzed with an inverted optical microscope, a series of initial tests over non-functionalized PDMS surfaces rapidly showed that their tailored functionalization with adhesion substrates, such as polyornithine, is a mandatory step to successfully achieve adhesion and survival of eukaryotes, such as hyppocampal cells, within microwells (see Fig 3.5).

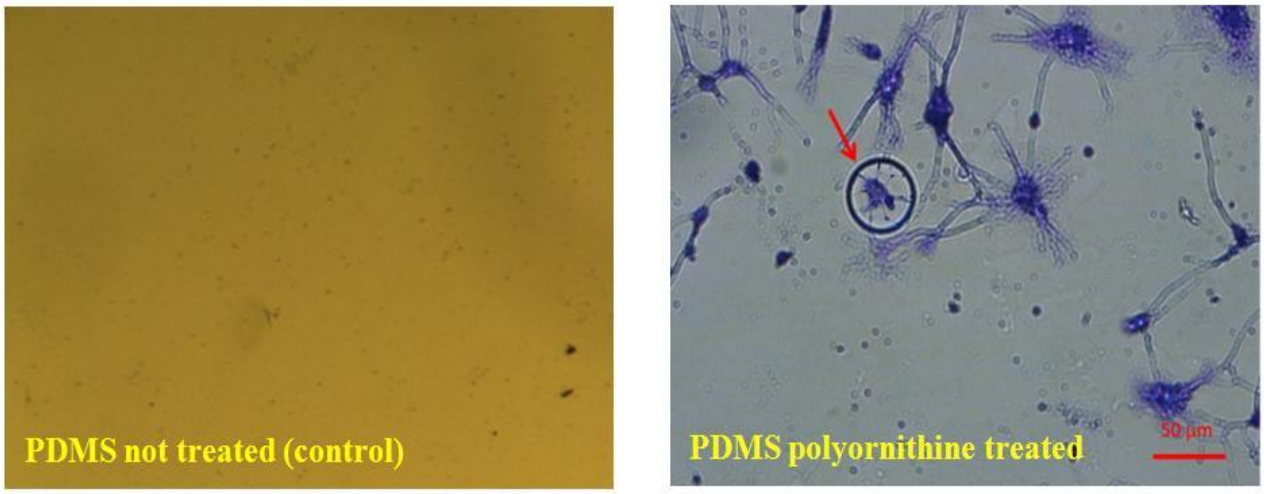

Fig 3.5: Patterning of hyppocampal cells on non-functionalized (left) and functionalized (right) PDMS surfaces.

The microcontact printing strategy exploited to functionalize the PDMS microwells yielded to a successful deposition of polyornithine only within the microwells: in fact the use of lucifer yellow to mark its presence nicely demonstrated their effective functionalization, as indicated by the fluorescent signal only in the well's floor and walls (see Fig 3.6).

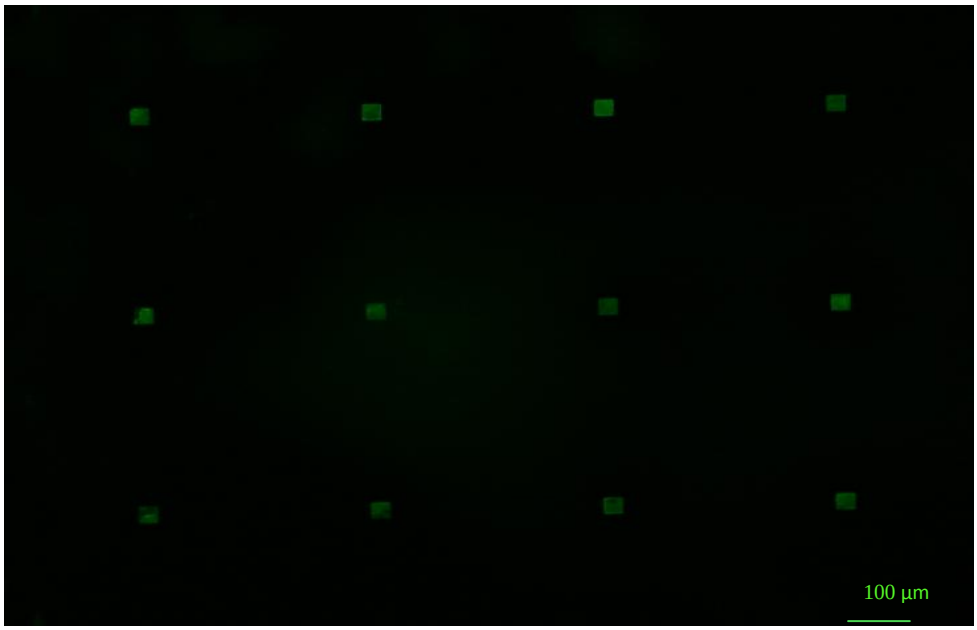

Fig 3.6: Functionalization of PDMS microwells with polyornithine stained in green thanks to lucifer yellow

In conclusion, these series of tests demonstrated that the microfabrication and functionalization processes are easily performed, and that they allow for a feasible and effective patterning of living CNS cells within PDMS microwells of the appropriate dimensions.

3.2 Optimizing the recognition of GFAP

As a first test meant to rule out any unspecific alteration of the TOEG SAMs (TOEG3 as well as TOEG6) after incubation with biological samples, 100µl of cells' lysate obtained firstly from prokaryotes (E.Coli) and lately from eukaryotes (HeLa cells) were deposited onto the SAMs, the incubation time lasted 1h at room temperature. Pre- and post-incubation imaging sessions were carried out throughout AFM-based roughness analysis in a solution of PBS 300µl with soft cantilevers (CSC 38, MikroMasch) and the following parameters: scan rate of 2000nm/s, pixel size 256 x 256.

These initial tests did not show any significant difference in terms of roughness of the SAMs as calculated before and after cell's lysate deposition, confirming the suitability of TOEG SAMs for their promising functionalization oriented toward effective nano-immuno recognition of the proteins of interest (see Table 3.1).

	Scan Size	Roughness Analysis	
		PBS	Cells' Lysate (1h)
TOEG3	1μm	155.7pm	143.1pm
	5μm	139.7pm	132.8pm
	10μm	135.7pm	143.0pm
TOEG6	1μm	145.2pm	132.0pm
	5μm	158.3pm	145.2pm
	10μm	147.5pm	148.5pm

Table 3.1: Physical properties (roughness) of TOEG surfaces are not altered after incubation with cell's lysate

3.2 a) Antibodies' immobilization

The fabrication of nanosized patches of biotin terminated alkanelthiol by AFM-based nanografting inside a matrix of SAM of alkanethiol-modified gold surfaces, rapidly yielded to a successful immobilization of biotinylated monoclonal GFAP Abs. On average the final NAMs' height was 11 ± 1nm, as confirmed by topographic imaging conducted in TBS with the AFM (see Fig 3.7).

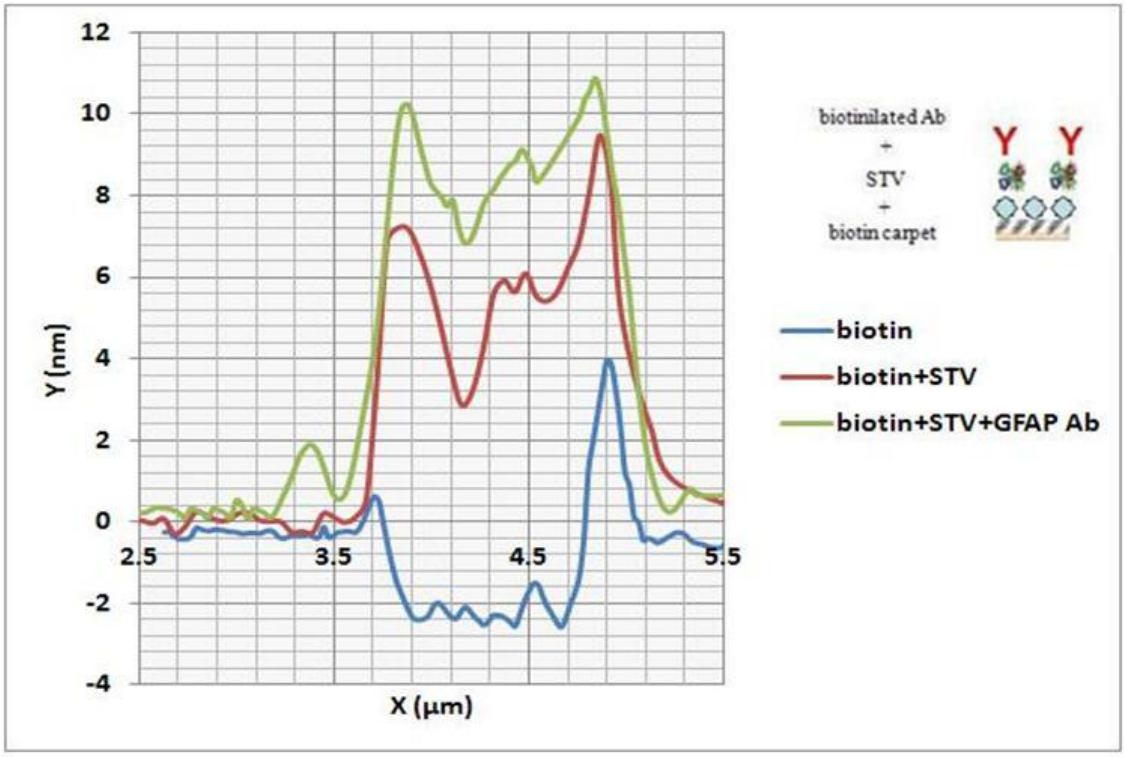

Fig 3.7: Successful immobilization of GFAP Abs onto NAMs of biotin terminated alkanethiol

Taking into account that the height of the TOEG6 monolayer, well known in our laboratory from extensive sets of previous measurements, ranges from 1.9nm to 2.1nm, each progressive increase, step by step observed, in the NAMs' relative height (Δh biotin+STV ≈ 6 nm and Δh GFAP Abs ≈ 3 nm) is compatible with crystallographic data (biotin+STV: 3nm x 6nm x 6nm; GFAP Abs 4nm x 2.5nm x 3nm) sorted from the literature according to Protein Data Bank (www.wwpdb.org).Noteworthy, the initial height of the biotin-modified alkanethiol (C_{16}) nanopatches was only ≈ 0.2nm, as calculated from the difference between the assumed TOEG6 height of 2.2nm and the measured difference of 2.0nm between $TOEG_6$ and the alkanethiol patch, and is certainly far too low for a standing-up alkanethiol monolayer. Nevertheless, since nanografting was performed in a water solution, and the used alkanethiol is not very soluble in water, what might have happened is that only few alkanethiol molecules were released in the nanografted area, probably adopting a laying-down conformation. Moreover, being the van der Waals radius of C ≈ 0.17nm, we should have expected to measure a 0.34nm absolute height after biotin terminated alkanethiol nanografting, so that a possible reason for this low initial height of the biotin-modified alkanethiol could probably be related to an excessive tip compression.

Although this strategy confirmed to be very effective and straightforward its unsuitability for multiplexing assays fostered the subsequent trials meant to optimize the DDI protocols for antibody/protein arrays. The first experiments testing the DDI strategy for immobilization of biotinylated Abs were carried out with cF4 ssDNA (5'-ctt att tta ttg tta tac gcc c-3') along with its cDNA already functionalized with a tyrosine binder-tag. Those tests led to progressive increase in the NAMs' height till to the hybridization of ssDNA with the STV-cDNA complex. In fact the binding between the tyrosin binder tag of the cF4 cDNA conjugate, and one of the 6 tyrosin chains of STV was obtained in solution before incubation with the ssDNA patches. As a result after immobilization of ssDNA and formation of the dsDNA+STV the measured relative height with regard to the TOEG monolayer were 6.8 ± 1.2nm and 13 ± 2.7nm respectively. Taking into account that the height of the TOEG monolayer ranges from 1.9nm to 2.1nm, we obtained an absolute height of the ssDNA of ≈ 8.7nm. The fully stretched length of a 24 nucleotides DNA, as the one used in this experiment, is expected to be ≈ 8.2nm + 1.2nm = 9.4nm, having taken into account the length of the C6 alkanethiol linker (1.2nm) attached to the ssDNA 3' termination. Following the study performed by Mirmomtaz and colleagues on variable density DNA patches, which correlates DNA patch height to DNA surface density (Mirmomtaz et al, 2008), we can conclude that our nanopatches had a concentration of molecules in the upper end of 10^{12}mol cm^{-2} range (probably. 7 - 9), and is definitely below saturation (3 x 10^{13} mol cm^{-2}). This condition corresponds to optimal

hybridization efficiency, and explains the correct formation of dsDNA-STV complexes (see Fig 3.8).

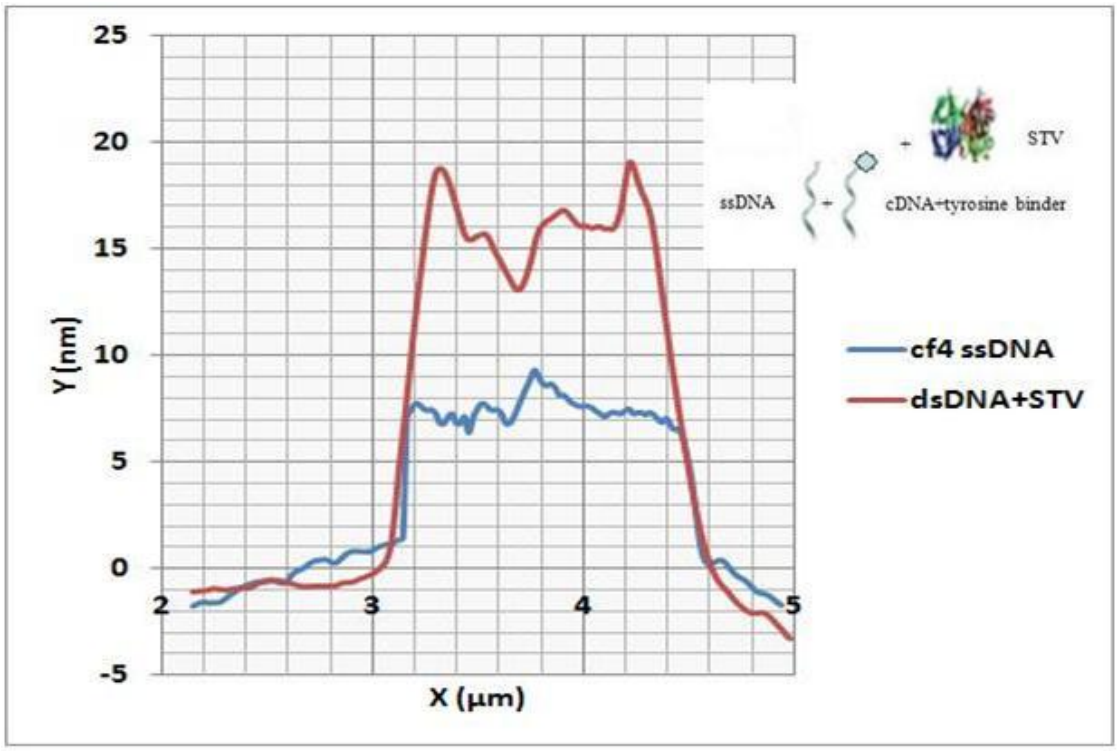

Fig 3.8: Successful hybridization of STV onto NAMs of cDNA with a tyrosin binder tag

Unfortunately none of the trials conducted with cF4 with the explained strategy yielded to a successful immobilization of biotinylated GFAP Abs: because of an uncontrollable lack of stability of those NAMs, the experiments were subsequently carried out with cF9 ssDNA (5'-ctt gat tgc cac ttt cca c-3') and its cDNA already functionalized with a STV-tag.

Nevertheless, those trials did not allow, initially, to obtain the hybridization between ssDNA and its conjugated-cDNA, instead a dramatic decrease in NAMs' height was always observed (see Fig 3.9).

To overcome this problem a similar strand of DNA, cF5 ssDNA (5'-ctt atc tta tga ccg gac c-3'), along with its cDNA already functionalized with a STV-tag was tried (see fig 3.10).

Even with this DNA strand the hybridization did not lead to an increase in NAMs' height as expected; instead those experiments confirmed as in the previous set with cF9 a decrease below initial ssDNA values. To understand the reasons for those failures each single step of the DDI protocol, its multiple parameters and every buffer utilized were independently assessed multiple times. Lastly, while struggling against these problems, concerns have been raised on the integrity of both the cDNA strands (cF9 and cF5) conjugated with STV.

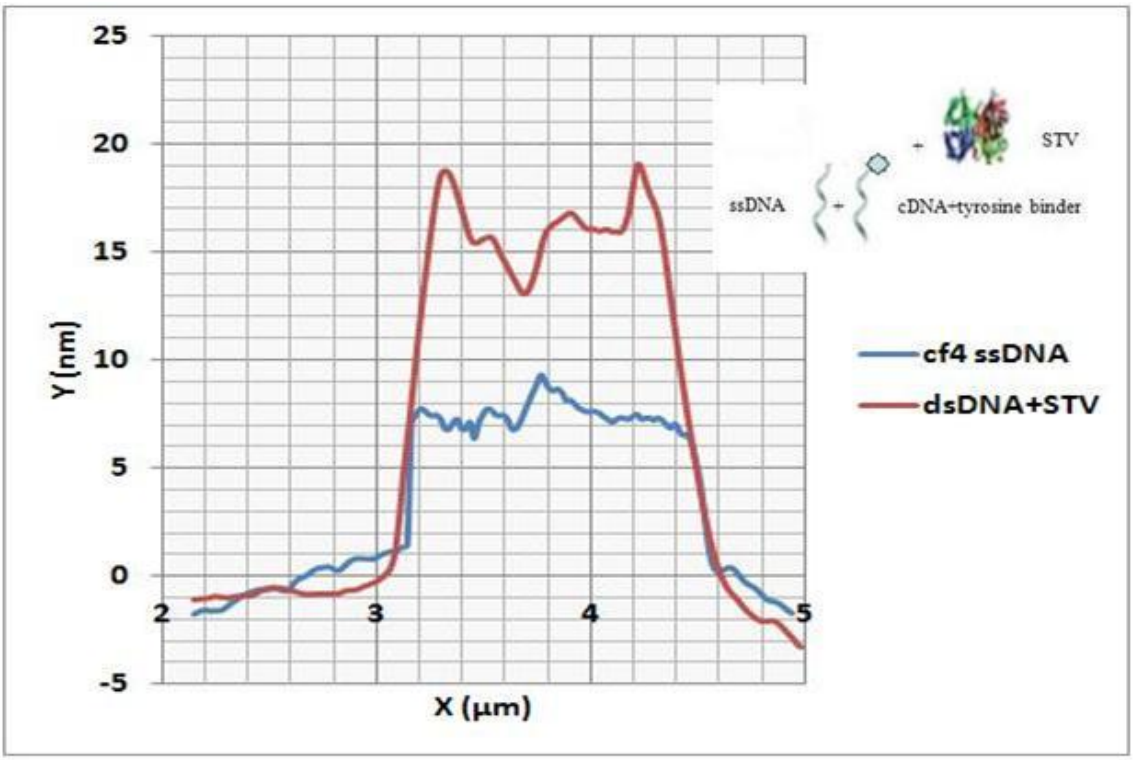

Fig 3.9: Decrease in the NAM's height following the tentative hybridization between cF9 ssDNA and its cDNA directly conjugated with STV

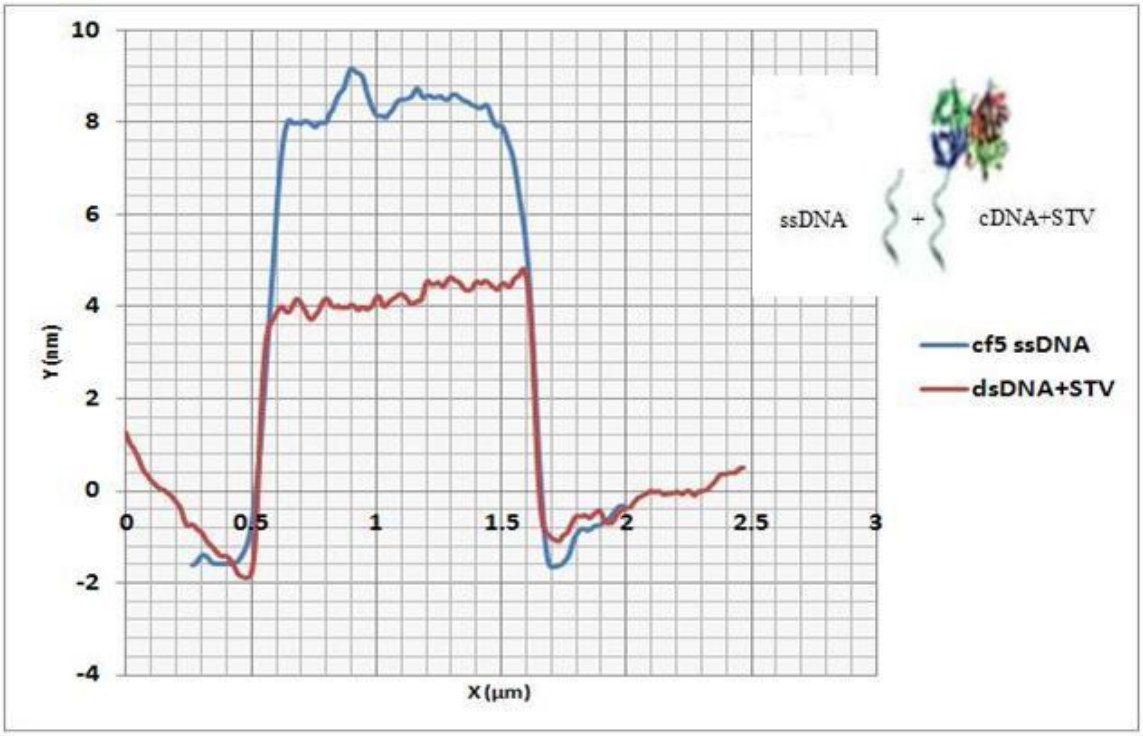

Fig 3.10: Decrease in the NAM's height following the tentative hybridization between cF5 ssDNA and its cDNA directly conjugated with STV

To test this hypothesis a Sodium Dodecyl Sulphate - PolyAcrylamide Gel Electrophoresis (SDS PAGE) assay, usually the first choice to assess protein purity due to its high reliability was conducted at the Structural Biology Lab @ Elettra.

Surprisingly, this SDS PAGE revealed a remarkable degradation of the STV tag, whose molecular weight is expected to be ≈ 60kDa (see Fig 3.11).

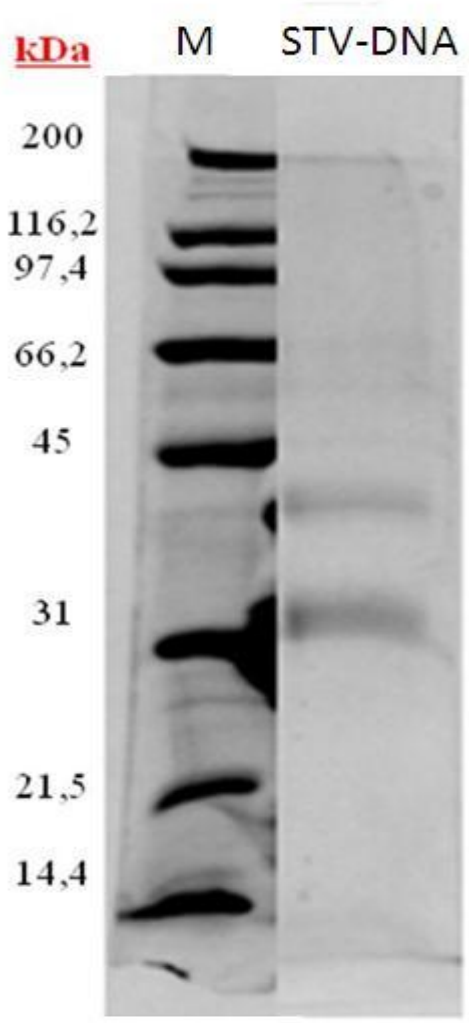

Fig 3.11: SDS PAGE of a DNA strand already functionalized with a STV-tag (right, note the absence of the expected STV stacking at 60kDa) versus control STV (left)

This result supported the internal speculations raised about the responsibility of the cDNA-STV construct, their possible degradation and consequent poor stability, for the failure of such set of experiments.

At the same time comforted by this SDS PAGE assay, we ruled out any doubt concerning the protocol itself.

The DDI strategy was therefore applied again, without changing the already optimized parameters but using a completely brand new batch of cF5 (5'-ctt att tta ttg tta tac gcc c-3') ssDNA and its freshly conjugated STV-cDNA (see Fig 3.12).

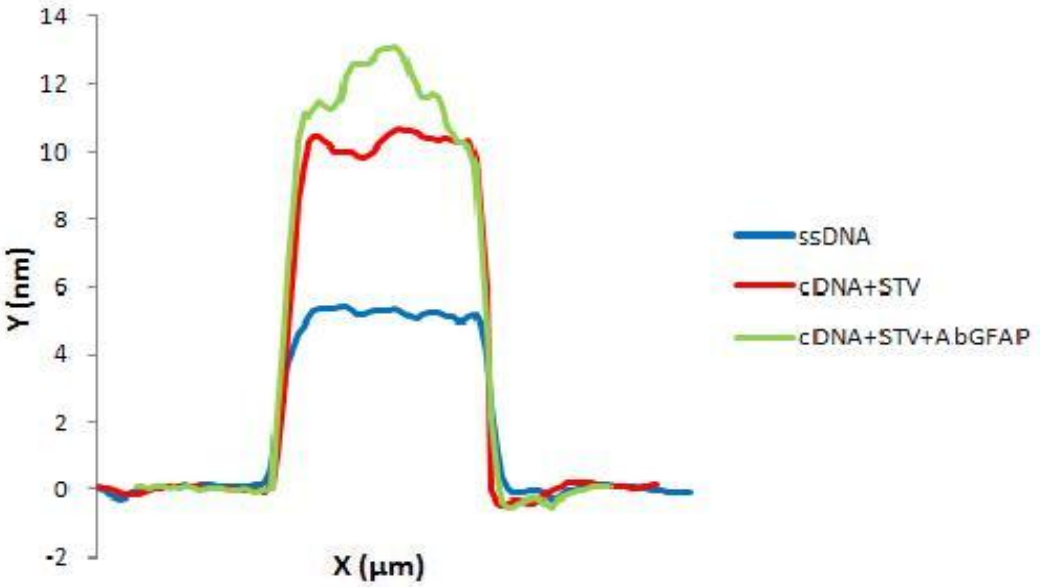

Fig 3.12: Successful immobilization of GFAP Abs onto DDI NAMs (imaging in TE)

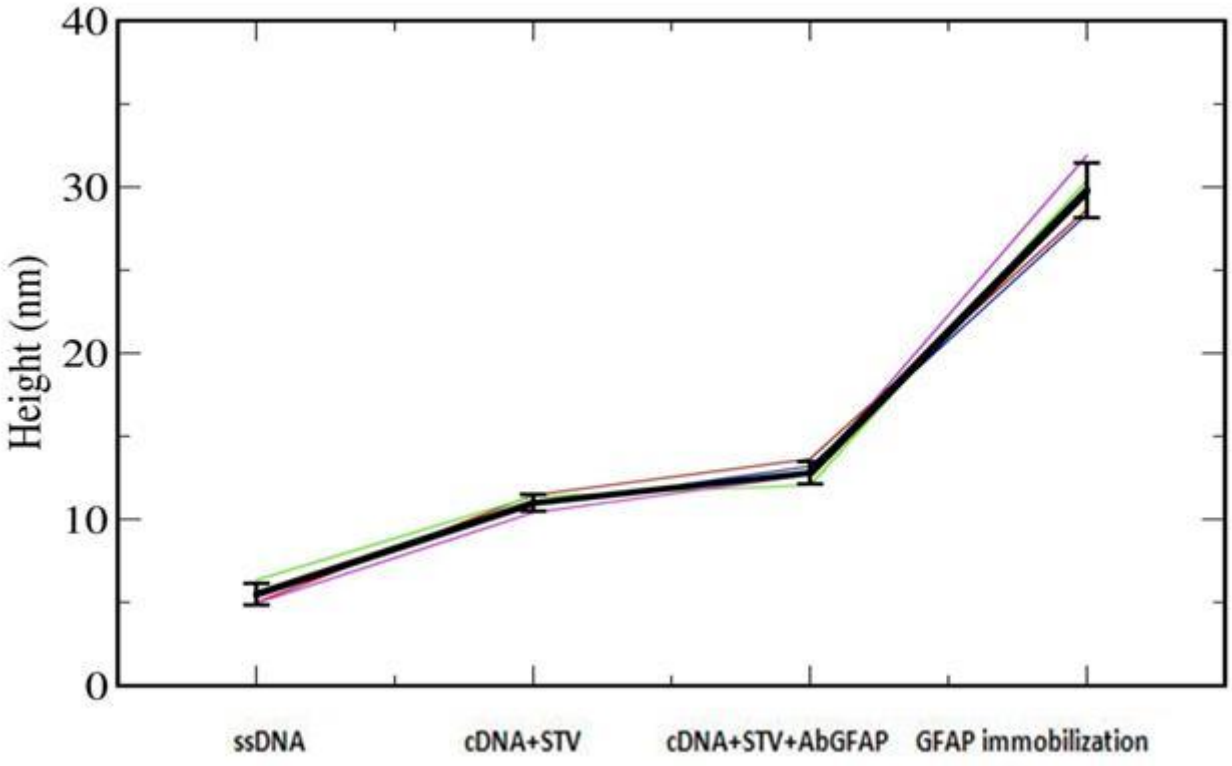

Fig 3.13: Progressive increase in NAMs' height in blocking buffer only (imaging in TE)

Those experiments yielded to a successful progressive increase in the relative NAM's height, on average from 5nm (ssDNA), to 10nm (cDNA+STV) till to 13nm (cDNA plus GFAP Abs) with respect to TOEG6.

Before proceeding to the experimental session dedicated to the recognition of GFAP, the behaviour of those NAMs was tested with biological samples in a multicells' lysate obtained from a eukaryote cell line (U87 glial culture). Accordingly the nano-immuno arrays were tested before and after functionalization with GFAP Abs by depositing on top of them 100µl of cells' lysate each time for 1h at room temperature.

Pre- and post-incubation imaging sessions were routinely carried out throughout AFM-based roughness analysis in a solution of PBS 300µl with soft cantilevers (CSC 38, MikroMasch) and the following parameters were applied: scan rate 2000nm/s, pixel size 256 x 256.

This experiment confirmed that the roughness of both NAMs and SAMs did not change significantly before and after incubation with cell's lysate, while the STV-tag of those NAMs still retain the specificity to appropriately immobilize biotinylated Abs (see Table 3.2).

TOEG6 SAM's Roughness Analyses w/wo cell's lysate

	Before incubation (Time 0)	After incubation (1 h)
cDNA+STV	0.2 ± 0.01 nm	0.2 ± 0.01 nm
cDNA+GFAP Ab	0.28 ± 0.01 nm	0.28 ± 0.01 nm

DDI NAM's Roughness Analyses w/wo cell's lysate

	Before incubation (Time 0)	After incubation (1 h)
cDNA+STV	1.3 ± 0.5 nm	1.3 ± 0.7 nm
cDNA+GFAP Ab	1.9 ± 0.5 nm	1.9 ± 0.8 nm

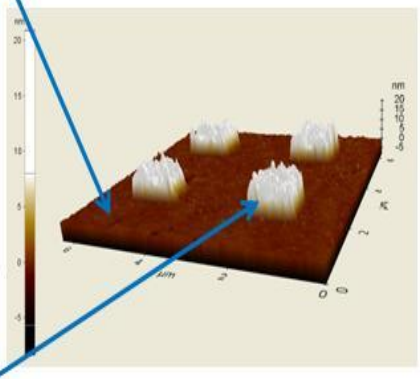

Table 3.2: Roughness Analysis with/without (w/wo) cell's lysate

After a long and continuous optimization of the DDI protocols, a better understanding of this strategy was finally achieved, developing a promising expertise in such a bottom up nanofabrication and nanofunctionalization technique.

Nevertheless, despite such encouraging results many aspects needed to be addressed: 1) the role of blocking buffers on the selectivity of the antigen antibody recognition, and 2) the ability of those NAMs to recognize the protein of interest in a cells' lysate.

3.2 b) GFAP in PBS

To verify the efficacy of blocking buffers to reduce the background noise or to prevent unspecific staining in presence of the ligand, the subsequent imaging sessions were always conducted in PBS, which is much more tailored for imaging of biologically active biosensors.

Noteworthy, when the experiment was repeated step by step, utilizing the abovementioned TBS buffer instead than TE (≈ 150mM), the progressive increases in relative height resulted slightly higher (see Figs 3.14 and 3.15). This result is conceivable since the two buffers have different ionic strengths: the higher is the ionic strength, the higher the screening of the electrostatic charge, the more the molecules adopt a compact conformation (i.e. lower height).

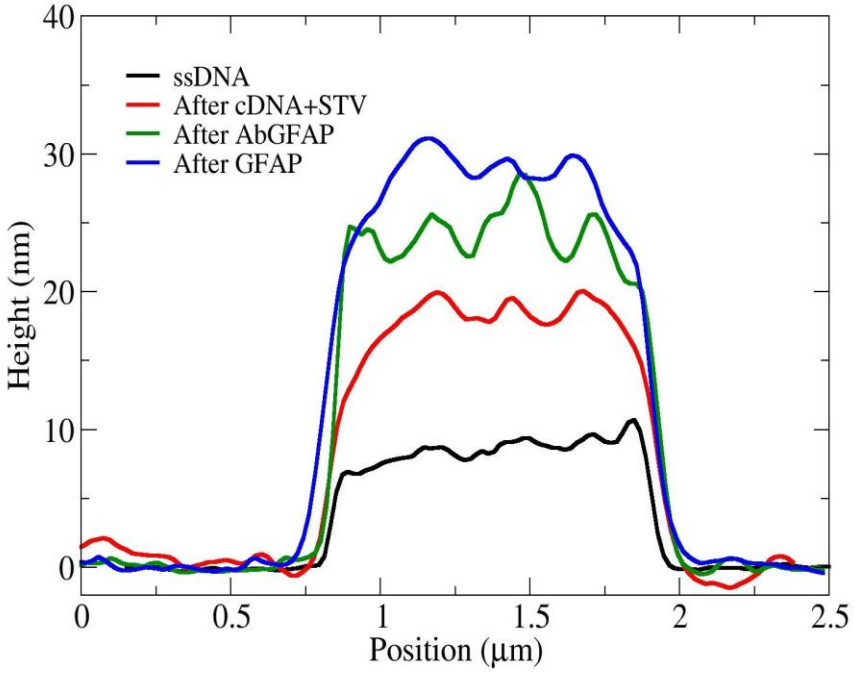

Fig 3.14: Successful immobilization of GFAP Abs onto DDI NAMs (imaging in TBS)

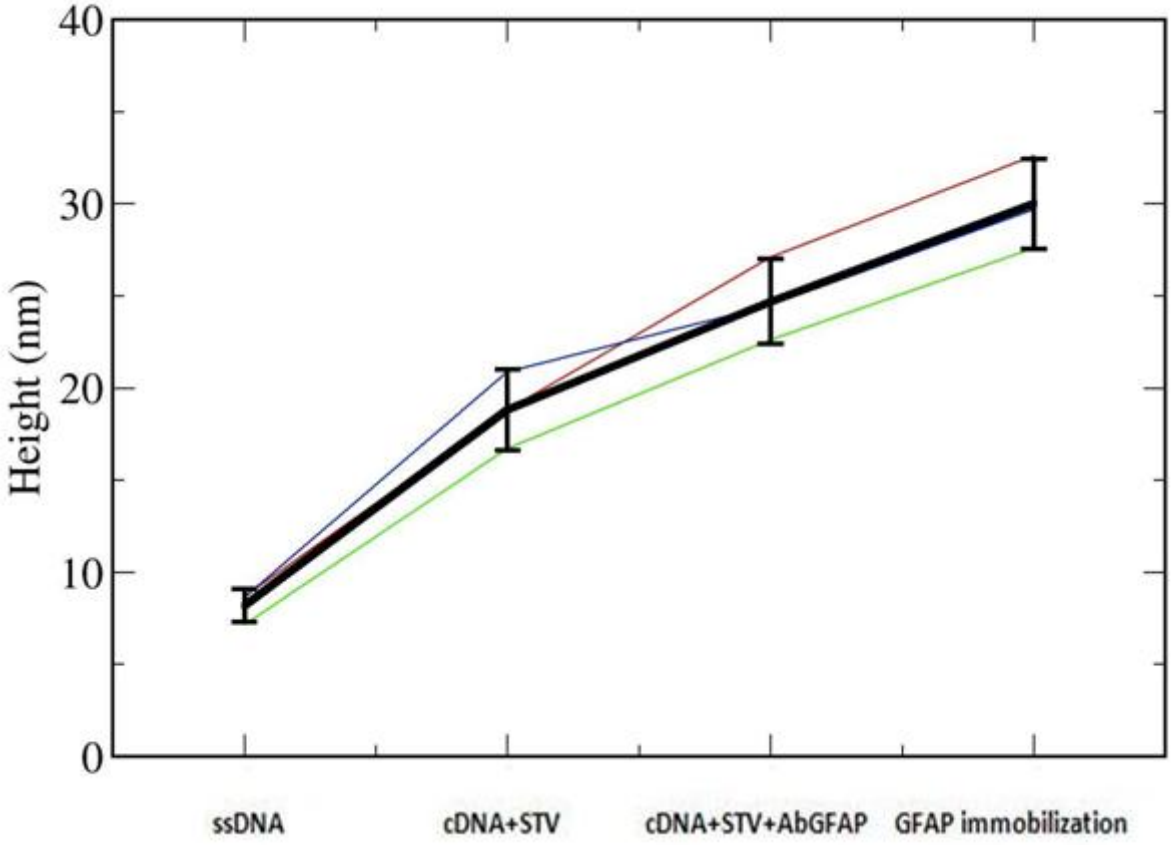

Fig 3.15: progressive increase in NAMs' height in blocking buffer (imaging in TBS)

3.2 c) GFAP in multicells' lysate

The suitability of those nano-immuno arrays to selectively recognize the protein of interest not only in presence of recombinant GFAP alone but also in the cells' proteome, which contains several different proteins potentially responsible for unspecific bindings over the NAMs or over the surrounding SAM, was finally tested by incubation of the SAM in a solution of 100µl of blocking buffer containing multicells' lysate (obtained from U87 cells at different concentration of 10^5cells/cc down to 10^4cells/cc) and recombinant GFAP at a known concentration of 40nM.

Starting from a relatively small, known concentration of 40nM, we observed that the final NAMs height corresponded to 32 ± 2.8nm, almost similar to the 29.4 ± 2.2nm registered in a solution of 100µl of blocking buffer containing only recombinant GFAP at a known concentration of 40nM (see Figs 3.16 and 3.17).

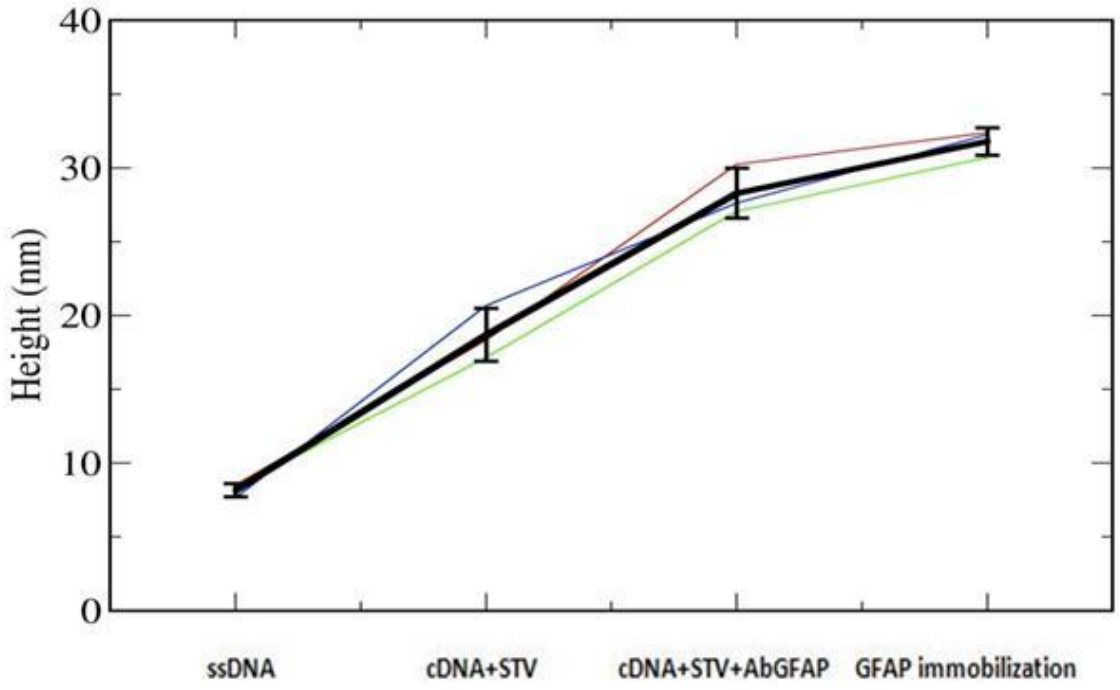

Fig 3.16: progressive increase in NAMs' height in blocking buffer plus multicells' lysate (imaging in TBS)

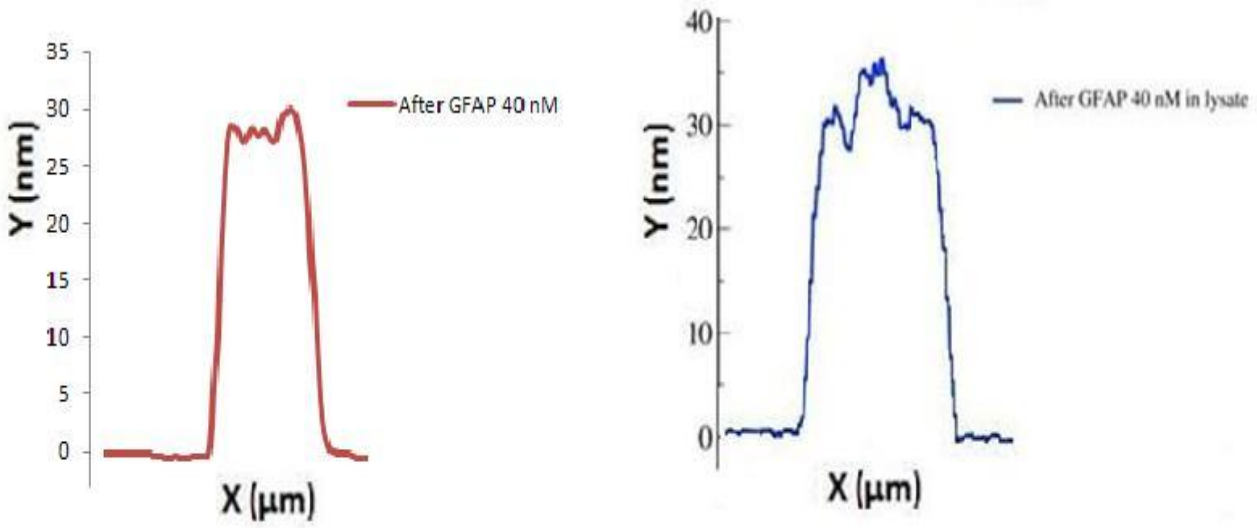

Fig 3.17: Final height of the nanopatches after incubation with recombinant GFAP in PBS and after incubation in the cells' proteome at the same concentration of GFAP (40nM)

Indeed, the evidence of a progressive NAMs' height increase confirmed the functionalized NAMs retain their selectivity in recognizing step by step the appropriate ligand. Moreover the 3-D images of the nano-immuno arrays, routinely obtained at the end of every step to check at a glance that the area surrounding each NAM was clean, suggested that the multicells' lysate did not influence nor the antigen-antibody recognition nor the subsequent height analysis (see Fig 3.18).

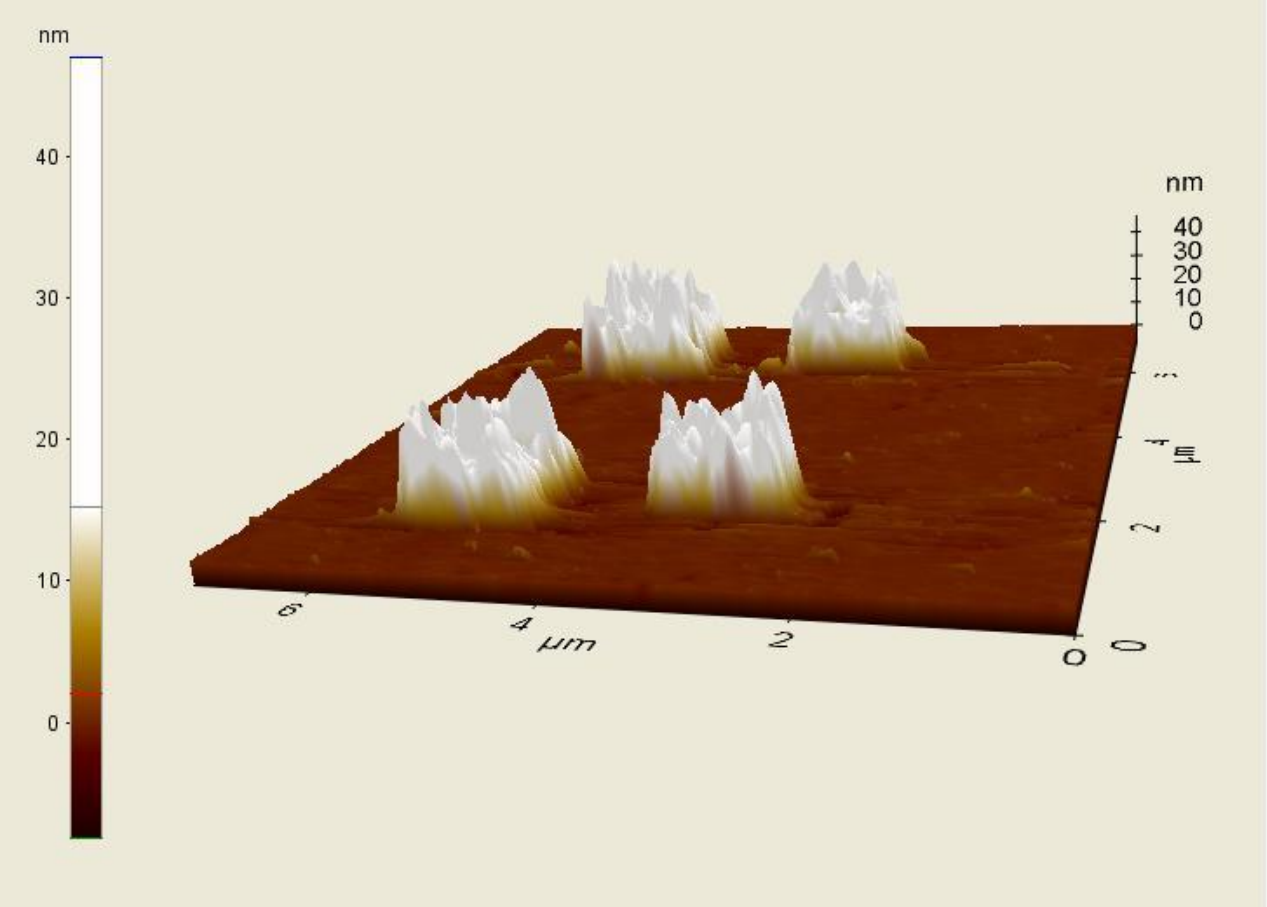

Fig 3.18: Successful recognition and immobilization of GFAP in multicells' lysate: both SAMs and NAMs are not affected by binding of unspecific proteins contained in the cells' lysate

Actually, the results herein presented confirm that on one hand, nanografting has unique capabilities for controlling density and conformation of patterned biomolecules at the nanometer scale; on the other, the inner characteristics of DDI, such as high efficiency of adsorption, site-selectivity and reversibility, allow for selective immobilization of a specific protein of interest on the generated DNA patterns using semisynthetic protein-DNA conjugates.

Once the proof of concept was obtained, a determination of the sensitivity of those nano-immuno arrays remained to be realized: for this reason we focused toward increasing the experimental data to realize a titration curve and compare it with that of ELISA.

3.3 Challenging the sensitivity of ELISA

Once optimized the antibody detection using a cells' lysate, we also decided to show the possibility to quantitatively determine the concentration of GFAP in the sample. We decided to obtain the affinity curve for our nanobiosensor assay by measuring the variation of the height on the biosensor after the incubation with a solution containing a fixed concentration of the protein of interest in blocking buffer. We therefore monitored the height variation on the patches topped with the GFAP Abs ranging from 200pM to 100nM showing a sigmoidal behaviour as expected for the binding of an antigen to antibody (see Fig 3.19).

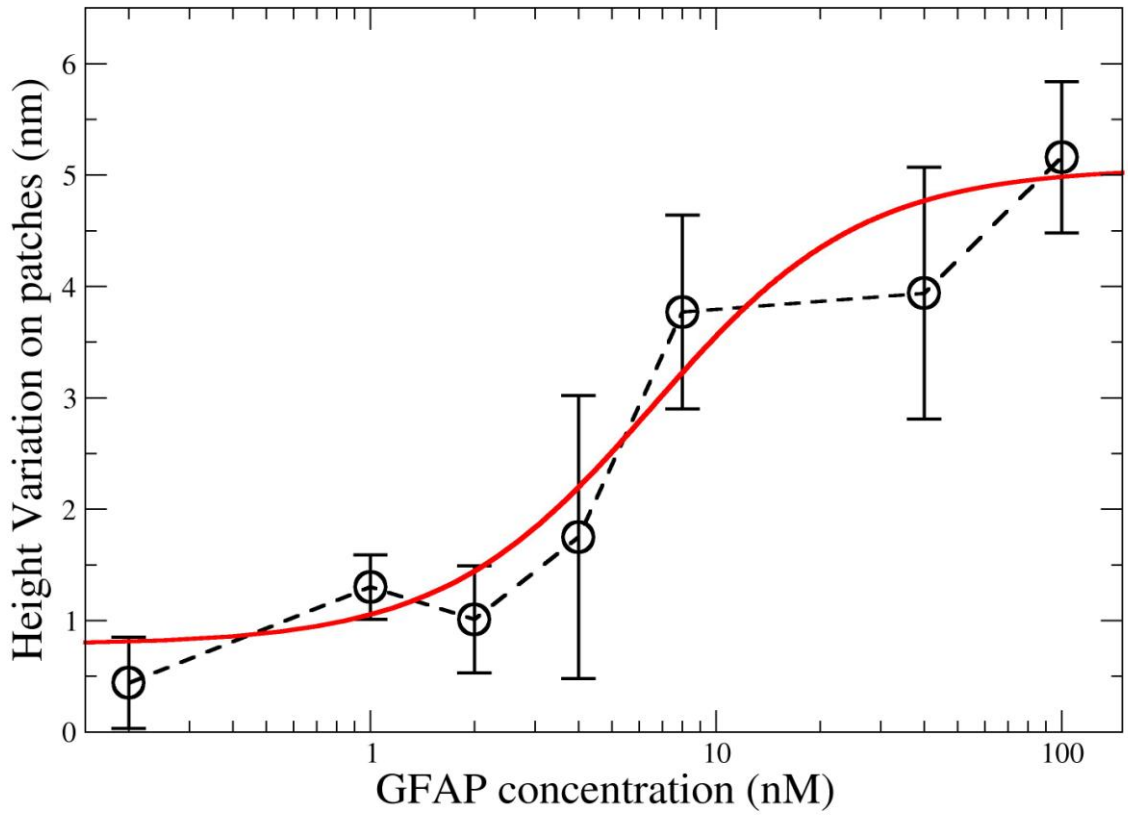

Fig 3.19: Titration curve of the nano-immuno arrays' sensitivity for GFAP. In black the experimental values (from 200pM to 100nM) and in red the fit with the Hill equation. From the fit we obtained: h_{min} *= 0.78 ± 0.28nm,* h_{max} *= 5.07 ± 0.75nm, n = 1.43 ± 0.82 and* K_D *= 6.6 ± 3.8nM*

In order to quantitatively describe the recognition of GFAP via our nanobiosensor assay, we utilized a standard sigmoidal curve (Hill equation) with the following formula:

$$\Delta h = h_{\min} + \frac{(h_{\max} - h_{\min})}{\left(\left({}^{[\mathrm{GFAP}]}/_{K_D}\right)^{-n} + 1\right)}$$

where $h_{\min}$ is the minimum height variation expected, $h_{\max}$ is the height variation upon saturation of our biosensor, K_D is the microscopic dissociation constant and n is the Hill coefficient that quantify the cooperativity of the binding.

From the fit, we obtained a dissociation constant in the nanomolar range, with a dissociation constant equal to K_D = 6.6 ± 3.8nM, and a slightly cooperative effect (n >1). However the large error in the Hill coefficient could mask the fact that the system has also a negative cooperative effect: meaning that once an antigene binds to an antibody, then the affinity of the antibody for another antigene decreases. In fact on our biosensor we expect that the steric hindrance between proximal Abs on the patches could contribute decreasing the cooperativity.

In order to study the binding affinity curve of our nanobiosensor assay with a standard technique, we produced an ELISA assay for GFAP using the same Abs (see Fig 3.20) and we analogously fit the values of absorbance with Hill equation.

The parameters obtained are n = 1.51 ± 0.26 that is compatible with a cooperative effect of the recognition event, and a dissociation constant equal to K_D = 8.30 ± 1.04nM that is perfectly in agreement with the value found for the nanosensor assay.

On a global perspective the results herein obtained are very promising: those data in particular allow envisioning the possibility for our nanodevice to be a valid alternative to ELISA assays.

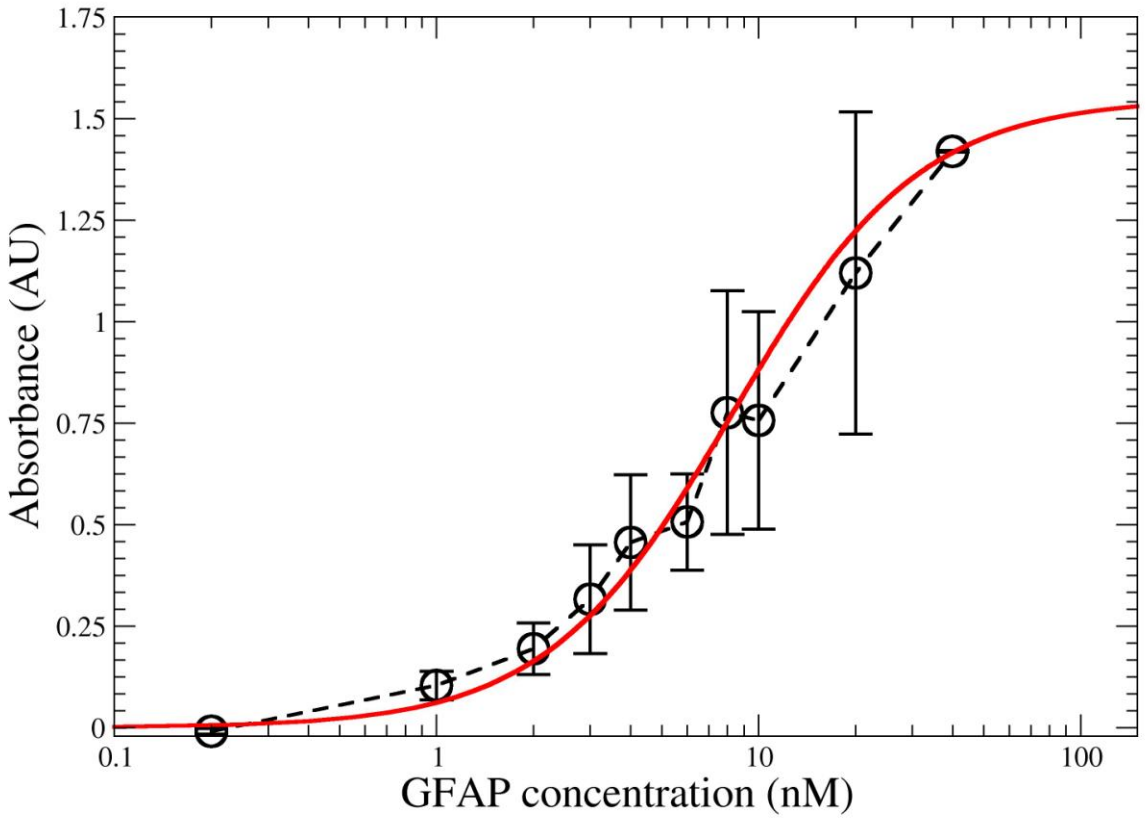

Fig 3.20: Sensibility of ELISA in GFAP recognition from 200pM to 100nM. In black the experimental values and in red the fit with the Hill equation. From the fit we obtained: Abs_{min} *= 0.00 ± 0.01,* Abs_{max} *= 1.55 ± 0.10, n = 1.51 ± 0.26 and* K_D *= 8.30 ± 1.04nM*

Chapter 4:

Discussion

4.1 Clinical Considerations

Clinicians are nowadays at a crossroad where therapeutic choices are being made not only considering conventional histological diagnosis but also the latest insights from molecular biology (Odreman et al, 2005). A significant body of evidence demonstrates that even genetically identical cells can exhibit significant functional heterogeneity, accordingly molecular cancer diagnostics is rapidly moving beyond genomics to proteomics, with the aim to identify those post-translational modifications expressed under pathologic conditions (Krutzik et al, 2004). The proteome and secretome by definition are dynamics and change both in physiologic and pathologic conditions; the ultimate goal of determining them is to characterize the flow of information within the cells, through the intercellular protein circuitry that regulates the extracellular microenvironment. Indeed, the study of proteomics and molecular biomarkers already allows to identify direct or indirect predictive factors, and soon it will hopefully determine which affected pathway could become a selective therapeutic target. Accordingly, nanotechnology-based approaches are being extensively explored to discover, identify and quantify clinically useful molecular signatures for early detection, diagnosis and prognosis of several tumors.

4.1 a) Genetic and Proteomic Features of Gliomas

One of the insidious biological features of gliomas is their potential to extensively invade normal brain tissue, yet molecular mechanisms that dictate this locally invasive behavior remain poorly understood (Ohgaki et al, 2005; Maruo et al, 2012).

To date many chromosomal and genetic aberrations involved in the genesis of high grade gliomas have been outlined, showing interesting relationships between survival, pathobiology, and molecular signature responsible for the formation of primary (de novo) and secondary (progressive) Glioblastomas (Mendoza-Maldonado et al, 2011) Although histologically indistinguishable, these WHO Grade IV tumors occur in different age groups and present distinct genetic alterations affecting similar molecular pathways (Brandes et al, 2010).

For example the inactivation of p53, a proapoptotic protein, may occur due to direct mutation in progressive Glioblastomas, or amplification of E3 ubiquitin-protein ligase Mdm2 (MDM2), a negative regulator of the p53 tumor suppressor gene, in de novo ones. Similarly, activation of the phosphonositide 3-kinase (PI3K) pathway, a family of enzymes involved in cellular functions such as cell growth, proliferation, differentiation, motility, survival and

intracellular trafficking, is induced by several cooperative mechanisms including: mutation of the tumor suppressor gene phosphatase and tensin homolog (PTEN), as well as epidermal growth factor receptor (EGFR) amplification and mutation (Furnari et al, 2007).

Immunohistochemical markers are therefore important and rapidly evolving tools in the classification and neuropathological diagnosis of malignant gliomas. Currently, among the markers for classification of gliomas, the most clinically useful and specific are GFAP and oligodendrocyte transcription factor 2 (OLIG2). In particular, GFAP is universally expressed in astrocytic and ependymal tumors and only rarely in oligodendroglial lineage tumors, thus serving as an effective tool for unequivocal identification of gliomas and their distinction from non-CNS tumors, while aiding the pathologist in the distinction of different glioma classes (Furnari et al, 2007).

The above described scenario gives an idea of the cellular and molecular complexity of the gliomas' microenvironment suggesting the importance to understand intracellular and intercellular signaling. Recently, an expanded collection of novel markers has emerged from numerous avenues of research and holds potential to be deployed to improve classification and inform the potential clinical course of glioma patients. Among them, newly discovered stem and progenitor cell markers are of particular interest because once clinically validated, they might aid in the differential diagnosis of these tumors as well as in the monitoring of their responses to therapy (see Fig 4.1).

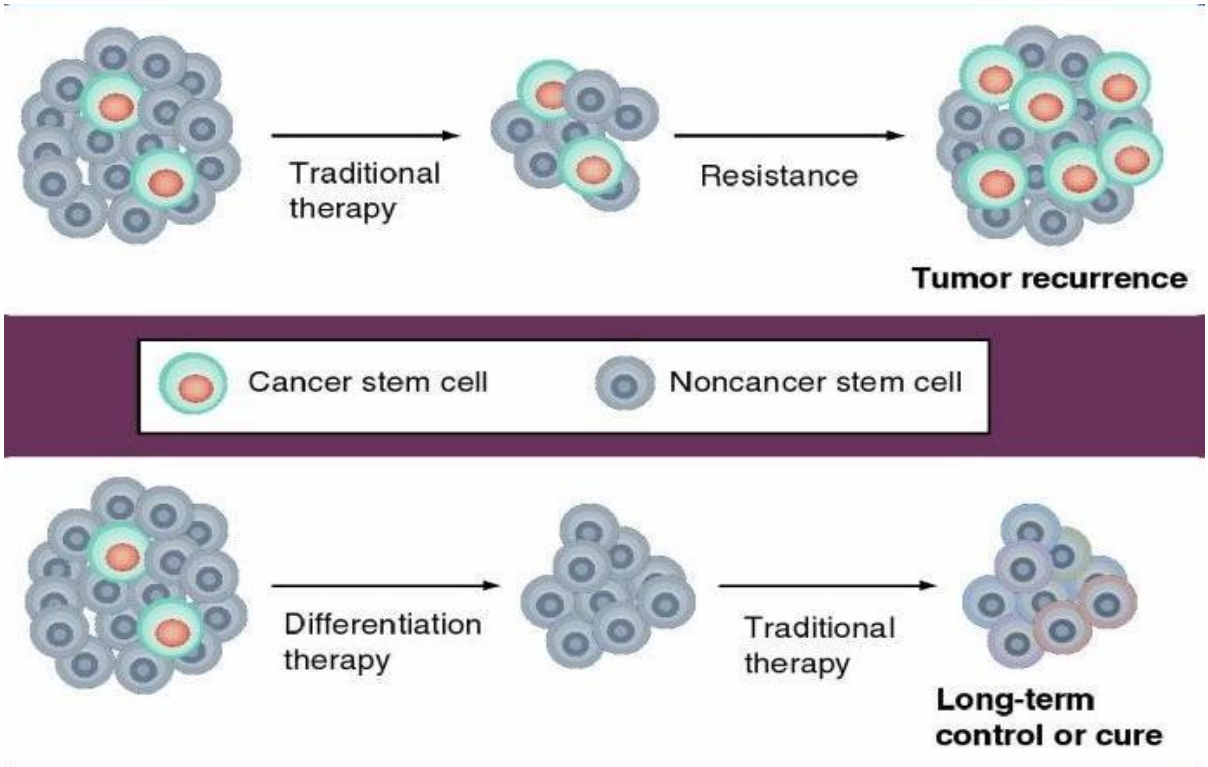

Fig 4.1: Role of stem cells in tumor recurrencies.

Drawing adapted from: Rahman M et al, Future Oncol 2012

Intensive research efforts are recently attempting to uncover agents that may target subpopulations of these cells with high tumorigenic potential and increased resistance to current therapies. Along these lines, the cell surface marker, CD133, and other markers of stem cells, such as Nestin, have been shown to negatively correlate with outcome parameters (Mao et al, 2007). To this regard Singh and colleagues showed that CD133+ brain tumor cells can self-renew and undergo lineage-specific differentiation (Singh et al, 2003). Certainly, these newly discovered markers suggest that pathologists will soon have at their disposal highly useful tools for improving the clinical diagnosis and classification of gliomas.

4.2 Methodological constraints and opportunities

Different ways to immobilize DNA molecules or specific proteins of interest have been subject of intensive research over the last years: the strongest efforts being put into the optimization of nano- to femtomolar detection of bioanalytes onto functionalized arrays surfaces. Understanding the structure and function of each protein and the complexities of protein–protein interactions will be critical for shaping the most effective proteomic instruments in the future. In general, among the complex aspects characterizing the development of biosensors the most intriguing one is certainly the individual conditioning of the different elements that must be assembled: proteins, DNA and antibodies must in fact maintain their functional conformation throughout the assay procedure, despite relevant differences in electrical charge, hydrophobicity, post-translational modification and folding (Ling et al, 2007). To date a number of techniques have emerged as effective tools for the discovery of key biomarkers, nevertheless a combination of multiple techniques is mandatory to attain the goal of measuring multiple parameters in a single living cell, and only the hybridization of proteomic methods with protocols and devices for cells patterning is finally yielding to the development of arrays for few cells proteomics.

4.2 a) DDI-based proteomic assays

Our approach utilized DNA self-assembly as a means to array antibodies specific for tumor biomarkers with well-defined size and spacing features. Such very general sensitive, reproducible, label free, miniaturized diagnostic platform seems particularly suitable for a parallel detection of 5 to 8 circulating tumor biomarkers, including cell-surface and intracellular biomarkers obtained *in*

vitro from tumor's lysate, or cytokines and other cell-signaling proteins detected *in vivo* from their secretome, in a quantitative manner and at a low cost (see Fig 4.2).

Due to the miniaturization and to its array format, our device can be easily made to face a microfabricated array of microwells with potentiality for single cells secretome analysis.

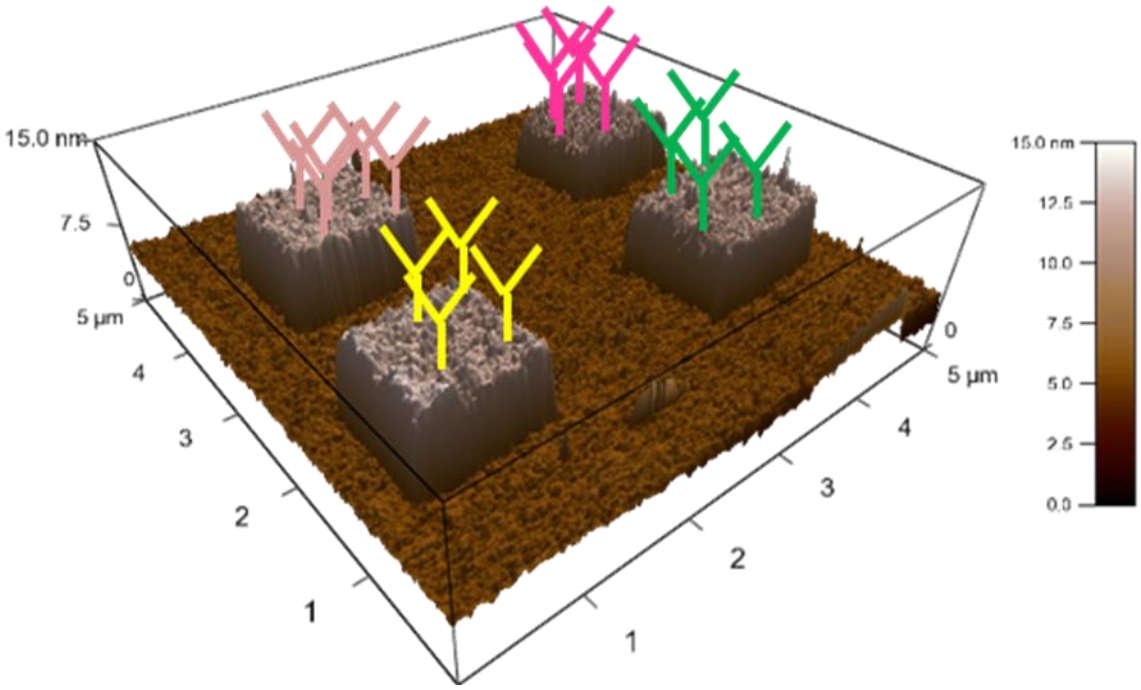

Fig 4.2: Intended functionalization of adjacent nano-immuno arrays for multiplexing analysis

Based on previous results obtained in our laboratory, we optimized the fabrication of DNA nano-immuno arrays as a first step towards the immobilization of Abs specific for certain proteins of interest, through an approach consisting in DDI of DNA-conjugated Abs. The device read-out consisted in AFM differential topographic height detection: upon binding of the target, the nanopatch height is expected to change, as a function of the number of biomolecules captured by the Abs on the nanospot. The feasibility of such kind of approach to detect, as a proof of principle, anti-streptavidin (STV) and anti-GoX (glucose oxidase) Abs was already experimentally demonstrated few years ago (Fruk et al, 2007; Bano et al, 2009), but only recently, we achieved the necessary expertise to successfully compare these nanodevices against standard ELISA assays on GFAP. With respect to ELISA, where the protein capture molecules are physisorbed on the surface and therefore randomly oriented, our assay shows unique capabilities for controlling and optimize density, binder directionality and to preserve its structural native conformation at the nanometer scale, with a strong impact on device sensitivity and reproducibility.

The binding affinity (titration) curves obtained to date from our nanobiosensor assay by measuring the variation of the height at the Abs-containing nanospot after the incubation with a solution containing a fixed concentration of the protein of interest in blocking buffer (following exactly the same protocols used for ELISA), confirms that the sensitivity of our nanosensors is at least that of ELISA, with the advantage of the scalability of the device.

Reducing the diffusion time of the solute, by exposing only the active area of the device to the solution (going to microliter to nanoliter), we could expect to easily increase the sensitivity of at least one order of magnitude. At this point, the optimization of the surface density of the DNA capture molecules on the device will be crucial. Experimental evidence that the hybridization limit of such nanodevices could be primarily and intrinsically controlled by molecular crowding are in fact arising.

4.2 b) Comparison with ELISA-based proteomic assays

The current standard for immunoassays and emerging molecular diagnostics is to analyze one analyte only: specifically, one aliquot of a patient sample (serum, plasma or tissue specimens) is processed and tested for one analyte at a time. Pressure for more accurate tests supported the extensive research to achieve state of the art performance of relatively simple assays.

As a reflection, ELISA is one of the most important bio-chemical techniques used mainly to detect the presence of Abs or antigens in a sample based on antibody-antigen immunoreactions (Jia et al, 2009).

Due to its simplicity, low cost, easy reading, acceptability and safety (Engvall and Perlman, 1971; Lequin et al 2005) ELISA is widely used for detection of cancer protein markers, pathogen, and other proteins relative to various diseases with detection limit from 0.1 ng to 1 $\mu g\ mL^{-1}$ (Engvall and Perlman, 1971; Koppelman et al, 2004).

However, the knowledge of specific tumor protein markers is still limited, especially for certain tumors such as high grade gliomas; on the other hand the level of those markers is very low at the early stage of several cancers and therefore beyond the detection limit of the state-of-the art diagnostic techniques.

Moreover, the demand for parallel, multiplex analysis of protein biomarkers from ever smaller biospecimens, such as those obtained with stereotaxis biopsies or after cell sorting of more abundant neoplastic specimens meant to identify tumor stem cells (i.e. CD133 glial cells), is an increasing trend for both fundamental biology and clinical diagnostics.

The need for increasing the current detection sensitivity, while searching for key proteins in smaller sample volumes, is therefore among the main triggering factors that led to the development of methods for single cells analyses. Attempts included miniaturization and mimicking of conventional proteomic protocols as well as exploration of novel ideas and techniques that enable new types of experiments, expanding the scientific field of "cells on a chip" in "single cells on a chip" (Lindstrom et al, 2011).

4.2 c) Trends in single cells DNA barcode analysis

The demand for parallel, multiplex analysis of protein biomarkers from even smaller biospecimens is an increasing trend for both fundamental biology and clinical diagnostics (Heath et al, 2008).

To date, the most highly multiplex protein assays rely on spatially encoded antibody microarrays, this approach capitalizes on the chemical robustness of DNA oligomer strands and on the reliable assembly of DNA labeled structures via complementary hybridization (Shin et al, 2010).

Recently the miniaturization of conventional techniques let to the development of DNA barcode-type arrays at 10-times higher density than standard spotted microarrays, potentially enabling for high-throughput and low-cost measurements.

Generally speaking, the immunoassay region of the chip should ideally be a microscopic barcode customized for the detection of many proteins and/or for the quantization of a single or few proteins over a broad concentration range.

Accordingly, using the DNA-encoded antibody library technique, Fan and colleague developed and optimized an antibody array applied towards the measurement of a highly multiplex panel of proteins from small whole blood specimens (range of μl obtained through finger prick).

The versatility of their barcode immunoassay is demonstrated by the ability to stratify cancer patients via multiple measurements of a dozen blood protein biomarkers for each patient (Fan et al, 2008).

This technique was further applied by coupling it with the immobilization of living cells, with an outlook for multiplex assay of citoplasmic proteins. Shin and colleagues for example, were able to detect simultaneously not only enzymes, such as phospho-extracellular signal regulated kinase (ERK), but also receptors, such as EGFR, both key nodes of the PI3K signaling pathway of glioblastomas, at concentrations of 10 to 1 ng/ml (Shin et al, 2010; Shi et al, 2012).

The coupling of DNA barcode analysis with immobilization and characterization of few to single cells represented a remarkable boost for cancer proteomics, in fact among the advantages of single cells analysis the main one is certainly the possibility to foster qualitative protein measurements, but in a quantitative fashion (Shi et al, 2012). One example relates to the interrogation of cross talk between signaling pathways within a cellular population as a paradigm to understand the overall tumor architecture: in their experiments Wang and colleagues assessed how cell-cell contacts and soluble factor signaling influence interaction among a glioma cell line (Wang et al, 2012).

In particular they interrogated the activity associated with PI3K signaling in a model of glioma cancer (U87 cells line) as a function of cell-cell separation: their results indicated that only a subpopulation of cells presented a constitutive activation of EGFR while the majority did not. This finding not only confirms that such approach allows for a thorough quantitative *in vitro* analysis of the proteome of few living cells, but also for a simulation of their hypothetical behavior *in vivo*: in line with the hypothesis that the expression of EGFR in a subpopulation of cells represents a trigger for parenchymal invasion, its expression if the majority of the entirety of the tumor would not enhance tumorigenicity instead would create a self-inhibiting state.

Hopefully, all these methodologies will soon increase the understanding of cellular pathways involved in high grade gliomas, so that tremendous advances might be expected within few years from now. With specific regard to the forthcoming steps of our research those advances could come on one hand from the exploitation of the potentialities for multiplexing analysis, demonstrated by our nanobiosensors, with concomitant detection of key biomarkers such as p53, nestin, EGF-R, OLIG2 or PTEN; on the other hand, aiming to increase the statistical value of the assays and therefore its clinical meaning, from the incubation of a relevant number of cells (hopefully $\approx$ 100, one for each microwell) obtained from homogeneous cell populations (perhaps sorted according to their positivity for CD 133).

Chapter 5:

Conclusions and Outlook

5.1 Optimization of protocols for protein recognition

The future of healthcare relies heavily on diagnostics: ideally, very early detection of unique molecular or protein patterns would allow for tailored treatments and management of many degenerative and neoplastic diseases (Stegh et al, 2013).

There are two main challenges in the development of new analytical methods for detection of proteins of interest: the first one is the technological, the second purely qualitative:

- The first technical challenge lies in reducing the quantities of biological specimens required for diagnostic assays, while scaling down the minimum amount of DNA or proteins that can be directly detected.
- The second consists in increasing the overall knowledge in the field of protein characterization and its clinical usefulness by identifying specific pathologic biomarkers and clarifying the correlation between over-expression or under-expression of certain proteins and the subsequent clinical course.

Indeed, the choice to optimize the DDI strategy, over the one consisting in the fabrication of nanosized patches of biotin terminated alkanethiol, was supported by the quest for multiplexing assays meant to overcome the current limits of single analyte assays. To this regard, the combination of nanografting with DDI meant for an easy, highly selective and precise arrangement of biomolecules, was already tested in a complex biological mixture represented by human serum (Bano et al, 2009); furthermore we have herein proved the ability of antibodies immobilized on the top of our nano-immuno arrays to preserve their specificity in the presence of a multicells' lysate.

Noteworthy, this strategy for realizing nano-immuno arrays seems particularly advantageous in terms of multiplexing analysis since the limiting factor for the number of protein tested is only the number of different DNA strands and antibody binding protein used. This technical feature could easily open the doors to future clinical applications of the diagnostic approach herein described. Especially because the accuracy achieved so far is a promising starting point to reach and eventually outreach the detection limits of ELISA protocols, while yielding to sensitivity maximization in term of sample quantities that are hardly accessible with conventional proteomic techniques.

Moreover, the inherent capacity of nucleic acids to self-assemble, exploited here, would also permit novel approaches based on the spontaneous formation of water-soluble, programmable nanoassemblies with defined shape, size and functionalities, as for DNA origami (Rothemund et al, 2006).

By introducing into our system a sandwich assay in which a second conjugated antibody, recognizing an independent epitope of the same protein, is combined via double-strand DNA interaction to a DNA-origami molecule modified with a fluorophore, we could combine the AFM topographic read-out to a fluorescence read-out. This approach could allow for fast screening and, perhaps for a further increase in the sensitivity of the system.

Also, fluorescence can be gauged in order to equalize the dynamic range of the fluorescence signals corresponding to biomarkers having different dynamic range of expression. Fluorescence-positive spots could then be analyzed by means of AFM topography read-out to check for eventual unspecific binding.

The main drawback of our technique could be seen then in the time needed for the process of nanografting itself. Nanografting is in fact a serial process that requires few hours to produce an ideal mesh of, for instance, 5x5 spots of $1\mu m^2$, meaning 5 different DNA to load 5 different antibodies, each one repeated 5 times for statistical purposes.

However, the DNA matrix produced by nanografting can be easily reproduced in multiple copies, by means of stamping techniques as SupraMolecular NanoStamping (Akbulut et al, 2007)**,** with the possibility of producing from one master some tens of copies of (negative) DNA matrixes.

Finally, in our system the technical ability of conjugate antibodies with DNA strand plays a major role, while the assay sensitivity is ultimately limited by the affinity of the chosen protein binder, i.e. the specific antibody-biomarker affinity. By choosing recombinant, single domain camel antibodies (in VHH format), having a mass of 15kDa (Aliprandi et al, 2010), which is 10-times smaller than a conventional IgG, more easy to functionalize or conjugate, we could prepare active surfaces with a significantly higher density, and we could identify Abs with optimal binding capacity for the *in vivo* receptor conformations, with the optimization of specific features (K_D and stability).

5.2 Toward Quantitative Neuroscience

The next generation of nanotechology-based devises hold the promise for improved multiplexed sensing and therefore for a better diagnostic accuracy meant to eventually improve the outcome of oncological patients. The results herein described represent an initial step to test the sensitivity and, in line with the expectation of a forthcoming patient-tailored medicine, the specificity of nano-immuno arrays designed for the detection of pivotal biomarkers, such as GFAP involved in the pathogenesis of gliomas. To this regard the characterization of this DDI strategy will

soon allow for the concomitant detection of several proteins of interest, making this technique a valid alternative for the current benchmark of ELISA-based proteomic.

Assaying a large panel of different proteins would not be possible without a high density antibody arrays, not just because they should be spatially constrained but also because of the high sensitivity required, therefore a consistent DNA loading across the nanoarray represents a meaningful strategy. The approach described of label-free nano-immuno detection, due to the promising results obtained in a multicells' lysate, confirms its suitability to effectively work in a complex environment without being influenced by unspecific bindings with the many elements included in a cell's proteome.

The biosensor configuration and the possibility to pattern living cells within functionalized microwells allows to easily enhance common proteomic strategies, with a successful clinical downstream. To this regard an appropriate design of the DNA nanospot in terms of probe density, length, etc, to maximize the hybridization efficiency with the DNA-protein conjugates, could be made with the aid of molecular simulations. Although further studies are warranted to better characterize the multiplexing strategy, this step seems easily reachable in the next future; a further clinical challenge will then be to expand this platform toward the analysis of surgical specimens, eventually including the comparison with conventional clinical and pathological data.

Abbreviation List

2DGE:	Two-dimensional gel electrophoresis
Abs:	Antibodies
AFM:	Atomic Force Microscopy
cDNA:	Complementary DNA strand
CNS:	Central Nervous System
DDI:	DNA-Directed-Immobilization
DPN:	Dip Pen Nanolithography
EDTA:	Ethylene-diamine-tetraacetic acid
EGFR:	Epidermal Growth Factor Receptor
ELISA:	Enzyme-linked immunosorbent assay
GFAP:	Glial Fibrillary Acidic Protein
HRP:	HorseRadish Peroxidase
IF:	Intermediate Filaments
MALDI-TOF:	Matrix-assisted laser desorption ionization time of flight mass spectrometry
MDM2:	E3 ubiquitin-protein ligase Mdm2
MGMT:	O(6)-methylguanine-DNA methyltransferase
NAM:	Nano Assembled Monolayer
OLIG2:	Oligodendrocyte Transcription Factor 2
PBS:	Phosphate Buffered Saline
PBST:	PBS + Tween 20

PDMS:	Poly-dimethylsiloxane
PI3K:	Phosphonositide 3-kinase
PTEN:	Phosphatase and Tensin Homolog
PVDF:	Polyvinylidene difluoride
SAM:	Self Assembled Monolayer
ssDNA:	Single Strand DNA
STV:	Streptavidine
TBS:	Tris Buffered Saline
TBST:	TBS + Tween 20
TE:	Tris-EDTA
TMZ:	Temozolomide
TOEG:	Alkanethiol-modified Gold
Tris:	Tris(hydroxymethyl)aminomethane

References

Akbulut O, Jung JM, Bennett RD, Hu Y, Jung HT, Cohen RE, Mayes AM, Stellacci F. Application of supramolecular nanostamping to the replication of DNA nanoarrays. *Nano Lett* 2007; 7(11): 3493-3498

Aliprandi M, Sparacio E, Pivetta F, Ossolengo G, Maestro R, de Marco A. The availability of a recombinant anti-SNAP antibody in VHH format amplifies the application flexibility of SNAP-tagged proteins. *J Biomed Biotechnol* 2010; 2010: 658954

Allen S, Chen X, Davies J, Davies MC, Dawkes AC, Edwards JC, Roberts CJ, Sefton J, Tendler SJ, Williams PM. Detection of antigen-antibody binding events with the atomic force microscope. *Biochemistry* 1997; 36(24): 7457-7463.

Arlett JL, Myers EB, Roukes ML. Comparative Advantages of Mechanical Biosensors. *Nat. Nanotechnol* 2011; 6: 203-215.

Bano F, Fruk L, Sanavio B, Glettenberg M, Casalis L, Niemeyer CM, Scoles G. Toward multiprotein nanoarrays using nanografting and DNA directed immobilization of proteins. *Nano Lett* 2009; 9: 2614-2618.

Bernard M, Renault JP, Michel B, Bosshard HR, Delamarche E. Microcontact printing of proteins. *Adv Mater* 2000; 12: 1067-1070

Bongcam-Rudloff E, Nistér M, Betsholtz C, Wang JL, Stenman G, Huebner K, Croce CM, Westermark B. Human glial fibrillary acidic protein: complementary DNA cloning, chromosome localization, and messenger RNA expression in human glioma cell lines of various phenotypes. *Cancer Res* 1991; 51: 1553-1560

Bosco A, Bano F, Parisse P, Casalis L, DeSimone A, Micheletti C. Hybridization in nanostructured DNA monolayers probed by AFM: theory versus experiment. *Nanoscale* 2012; 4(5): 1734-1741

Brandes AA, Franceschi E, Tosoni A, Bartolini S, Bacci A, Agati R, Ghimenton C, Turazzi S, Talacchi A, Skrap M, Marucci G, Volpin L, Morandi L, Pizzolitto S, Gardiman M, Andreoli A, Calbucci F, Ermani M. O(6)-methylguanine DNA-methyltransferase methylation status can change between first surgery for newly diagnosed glioblastoma and second surgery for recurrence: clinical implications. *Neuro Oncol* 2010; 12(3): 283-288

Cairncross JG, Ueki K, Zlatescu MC, Lisle DK, Finkelstein DM, Hammond RR, Silver JS, Stark PC, Macdonald DR, Ino Y. Specific genetic predictors of chemotherapeutic response and survival in patients with anaplastic oligodendrogliomas. *J. Natl. Cancer Inst* 1998; 90: 1473-1479.

Castronovo M, Scaini D. The atomic force microscopy as a lithographic tool: nanografting of DNA nanostructures for biosensing applications. *Methods Mol Biol* 2011; 749: 209-221

Chai J, Wong LS, Giam L, Mirkin CA. Single-molecule protein arrays enabled by scanning probe block copolymer lithography. *Proc Natl Acad Sci USA* 2011; 108(49): 19521-19525

Czerkinsky CC, Nilsson LA, Nygren H, Ouchterlony O, Tarkowski A. A solid-phase enzyme-linked immunospot (ELISPOT) assay for enumeration of specific antibody-secreting cells. *J Immunol Methods* 1983; 65(1-2): 109-121

Deng L, Broom A, Kitova EN, Richards MR, Zheng RB, Shoemaker GK, Meiering EM, Klassen JS. Kinetic stability of the streptavidin-biotin interaction enhanced in the gas phase. *J Am Chem Soc.* 2012; 134(40): 16586-16596.

Eng LF, Ghirnikar RS, Lee YL. Glial fibrillary acidic protein: GFAP-thirty-one years (1969-2000). *Neurochem Res* 2000; 25: 1439-1451.

Fan R, Vermesh O, Srivastava A, Yen BK, Qin L, Ahmad H, Kwong GA, Liu CC, Gould J, Hood L, Heath JR. Integrated barcode chips for rapid, multiplexed analysis of proteins in microliter quantities of blood. *Nat Biotechnol* 2008; 26(12): 1373-1378.

Fine HA, Dear KB, Loeffler JS *et al.* Meta-analysis of radiation therapy with and without adjuvant chemotherapy for malignant gliomas in adults. *Cancer* 1993; 71: 2585-97

Freije WA, Castro-Vargas FE, Fang Z, Horvath S, Cloughesy T, Liau LM, Mischel PS, Nelson SF. Gene expression profiling of gliomas strongly predicts survival. *Cancer Res* 2004; 64: 6503-6510.

Fruk L, Müller J, Weber G, Narváez A, Domínguez E, Niemeyer CM. DNA-directed immobilization of horseradish peroxidase-DNA conjugates on microelectrode arrays: towards electrochemical screening of enzyme libraries. *Chemistry* 2007; 13(18): 5223-5231

Furnari FB, Fenton T, Bachoo RM, Mukasa A, Stommel JM, Stegh A, Hahn WC, Ligon KL, Louis DN, Brennan C, Chin L, DePinho RA, Cavenee WK. Malignant astrocytic glioma: genetics, biology, and paths to treatment. Genes Dev 2007; 21: 2683-2710

Godovac-Zimmermann J, Kleiner O, Brown LR, Drukier AK. Perspectives in spicing up proteomics with splicing. *Proteomics* 2005; 5(3): 699-709

Heath JR, Davis ME. Nanotechnology and cancer. *Annu Rev Med* 2008; 59: 251-265.

Husain H, Savage W, Grossman SA, Ye X, Burger PC, Everett A, Bettegowda C, Diaz LA Jr, Blair C, Romans KE, Holdhoff M. Pre- and post-operative plasma glial fibrillary acidic protein levels in patients with newly diagnosed gliomas. *J Neurooncol* 2012; 109: 123-127.

Kingsmore SF. Multiplexed protein measurement: technologies and applications of protein and antibody arrays. *Nat Rev Drug Discov* 2006; 5(4): 310-320.

Kitange GJ, Templeton KL, and Jenkins RB. Recent advances in the molecular genetics of primary gliomas. *Curr. Opin. Oncol* 2003; 15: 197-203.

Kleiner O, Price DA, Ossetrova N, Osetrov S, Volkovitsky P, Drukier AK, Godovac-Zimmermann J. Ultra-high sensitivity multi-photon detection imaging in proteomics analyses. *Proteomics* 2005; 5(9): 2322-2330

Krutzik PO, Irish JM, Nolan GP, Perez OD. Analysis of protein phosphorylation and cellular signaling events by flow cytometry: techniques and clinical applications. *Clin Immunol* 2004; 110(3): 206-221

Kumar A, Whitesides GM. Features of gold having micrometer to centimeter dimensions can be formed through a combination of stamping with an elastomeric stamp and an alkanethiol ink followed by chemical etching. *App. Phys. Lett.* 1993; 63: 2002-2004

Kusnezow W, Syagailo YV, Goychuk I, Hoheisel JD, Wild DG. Antibody Microarrays: The Crucial Impact of Mass Transport on Assay Kinetics and Sensitivity. *Expert Rev Mol Diagn* 2006; 6: 111-124

Lechapt-Zalcman E, Levallet G, Dugué AE, Vital A, Diebold MD, Menei P, Colin P, Peruzzy P, Emery E, Bernaudin M, Chapon F, Guillamo JS. O(6) -methylguanine-DNA methyltransferase (MGMT) promoter methylation and low MGMT-encoded protein expression as prognostic markers in glioblastoma patients treated with biodegradable carmustine wafer implants after initial surgery followed by radiotherapy with concomitant and adjuvant temozolomide. *Cancer* 2012; 118(18): 4545-4554

Lees JE, Richards PG. Rapid, high-sensitivity imaging of radiolabeled gels with microchannel plate detectors. *Electrophoresis* 1999; 20(10): 2139-2143

Li HW, Muir BVO, Fichet G, Huck WTS. Nanocontact Printing: A Route to Sub-50-nm-Scale Chemical and Biological Patterning. *Langmuir* 2003; 19: 1963-1965

Liang J, Castronovo M, Scoles G. DNA as invisible ink for AFM nanolithography. *J Am Chem Soc* 2012; 134(1): 39-42.

Liedtke W, Edelmann W, Bieri PL, Chiu FC, Cowan NJ, Kucherlapati R, Raine CS. GFAP is necessary for the integrity of CNS white matter architecture and long-term maintenance of myelination. *Neuron* 1996; 17: 607-615.

Ling MM, Ricks C, Lea P. Multiplexing molecular diagnostics and immunoassays using emerging microarray technologies. *Expert Rev Mol Diagn* 2007; 7(1): 87-98.

Liu M, Amro NA, Liu GY. Nanografting for surface physical chemistry. *Annu Rev Phys Chem* 2008; 59: 367-386

Liu M, Liu GY. Hybridization with nanostructures of single-stranded DNA. *Langmuir* 2005; 21(5): 1972-1978

López GP, Biebuyck HA, Frisbie CD, Whitesides GM. Imaging of features on surfaces by condensation figures. *Science* 1993; 260(5108): 647-649

Mao Y, Zhou L, Zhu W, Wang X, Yang G, Xie L, Mao X, Jin K. Proliferative status of tumor stem cells may be correlated with malignancy grade of human astrocytomas. *Front Biosci* 2007; 12: 2252-2259

Maruo T, Ichikawa T, Kanzaki H, Inoue S, Kurozumi K, Onishi M, Yoshida K, Kambara H, Ouchida M, Shimizu K, Tamaru S, Chiocca EA, Date I. Proteomics-based analysis of invasion-related proteins in malignant gliomas. *Neuropathology* 2012; doi: 10.1111/j.1440-1789.2012.01361.x. [Epub ahead of print]

Melli M, Scoles G, Lazzarino M. Fast detection of biomolecules in diffusion-limited regime using micromechanical pillars. *ACS Nano* 2011; 5(10): 7928-7935

Mendoza-Maldonado R, Faoro V, Bajpai S, Berti M, Odreman F, Vindigni M, Ius T, Ghasemian A, Bonin S, Skrap M, Stanta G, Vindigni A. The human RECQ1 helicase is highly expressed in glioblastoma and plays an important role in tumor cell proliferation. *Mol Cancer* 2011; 10: 83

Mirkin CA, Letsinger RL, Mucic RC, Storhoff JJ. A DNA-based method for rationally assembling nanoparticles into macroscopic materials. *Nature* 1996; 382(6592): 607-609

Mirmomtaz E, Castronovo M, Grunwald C, Bano F, Scaini D, Ensafi AA, Scoles G, Casalis L. Quantitative study of the effect of coverage on the hybridization efficiency of surface-bound DNA nanostructures. *Nano Lett* 2008; 8(12): 4134-4139

Moncada V, Srivastava S. Biomarkers in oncology research and treatment: early detection research network: a collaborative approach. *Biomark Med* 2008; 2(2): 181-195.

Nair PR, Alam MA. Performance Limits of Nanobiosensors. *Appl Phys Lett* 2006; 88: 233120

Niemeyer CM, Sano T, Smith CL, Cantor CR. Oligonucleotide-directed self-assembly of proteins: semisynthetic DNA--streptavidin hybrid molecules as connectors for the generation of macroscopic arrays and the construction of supramolecular bioconjugates. *Nucleic Acids Res* 1994; 22(25): 5530-5539

Niemeyer CM, Boldt L, Ceyhan B, Blohm D. DNA-Directed immobilization: efficient, reversible, and site-selective surface binding of proteins by means of covalent DNA-streptavidin conjugates. *Annal Biochem*. 1999; 268(1): 54-63.

Niemeyer CM. The developments of semisynthetic DNA-protein conjugates. *Trends Biotechnol* 2002; 20(9): 395-401

Niemeyer CM. Semisynthetic DNA-protein conjugates for biosensing and nanofabrication. *Angew Chem Int Ed Engl* 2010; 49(7): 1200-1216

Nutt CL, Mani DR, Betensky RA, Tamayo P, Cairncross JG, Ladd C, Pohl U, Hartmann C, McLaughlin ME, Batchelor TT. Gene expression-based classification of malignant gliomas correlates better with survival than histological classification. *Cancer Res* 2003; 63: 1602-1607

Odreman F, Vindigni M, Gonzales ML, Niccolini B, Candiano G, Zanotti B, Skrap M, Pizzolitto S, Stanta G, Vindigni A. Proteomic studies on low- and high-grade human brain astrocytomas. *J Proteome Res* 2005; 4(3): 698-708

Ohgaki H, Dessen P, Jourde B et al. Genetic pathways to glioblastoma: a population based study. *Cancer Res* 2005; 64: 6892-99

Ohgaki H, Kleihues P. Population based studies on incidence, survival rates, and genetic alterations in astrocytic and oligodendroglial gliomas. *J Neuropathol Exp Neurol* 2005; 64: 479-89

Picas L, Milhiet PE, Hernández-Borrell J. Atomic force microscopy: a versatile tool to probe the physical and chemical properties of supported membranes at the nanoscale. *Chem Phys Lipids* 2012; 165(8): 845-860

Piner RD, Zhu J, Xu F, Hong S, Mirkin CA. "Dip-Pen" nanolithography *Science* 1999; 283(5402):661-663

Prados MD, Levin V. Biology and treatment of malignant glioma. *Semin. Oncol* 2000; 27: 1-10.

Rahman M, Hoh B, Kohler N, Dunbar EM, Murad GJ. The future of glioma treatment: stem cells, nanotechnology and personalized medicine. *Future Oncol* 2012; 8(9): 1149-1156.

Rasooly A, Jacobson J. Development of biosensors for cancer clinical testing. *Biosens Bioelectron* 2006; 21(10): 1851-1858.

Rothemund PW. Folding DNA to create nanoscale shapes and patterns. *Nature* 2006; 440(7082): 297-302.

Rusling JF, Kumar CV, Gutkind JS, Patel V. Measurement of biomarker proteins for point-of-care early detection and monitoring of cancer. *Analyst* 2010; 135(10): 2496-2511.

Sanavio B, Scaini D, Grunwald C, Legname G, Scoles G, Casalis L. Oriented immobilization of prion protein demonstrated via precise interfacial nanostructure measurements. *ACS Nano* 2010; 4(11): 6607-6616.

Schena M, Shalon D, Davis RW, Brown PO. Quantitative monitoring of gene expression patterns with a complementary DNA microarray. *Science* 1995; 270(5235): 467-470.

Sheehan PE, Whitman LJ. Detection Limits for Nanoscale Biosensors. *Nano Lett* 2005; 5: 803-807

Shi Q, Qin L, Wei W, Geng F, Fan R, Shin YS, Guo D, Hood L, Mischel PS, Heath JR. Single-cell proteomic chip for profiling intracellular signaling pathways in single tumor cells. *Proc Natl Acad Sci U S A* 2012; 109(2): 419-424.

Shin YS, Ahmad H, Shi Q, Kim H, Pascal TA, Fan R, Goddard WA 3rd, Heath JR. Chemistries for patterning robust DNA microbarcodes enable multiplex assays of cytoplasm proteins from single cancer cells. *ChemPhysChem* 2010; 11(14): 3063-3069.

Singh SK, Clarke ID, Terasaki M, Bonn VE, Hawkins C, Squire J, Dirks PB. Identification of a cancer stem cell in human brain tumors. *Cancer Res* 2003; 63; 5821-5828

Stegh AH. Toward personalized cancer nanomedicine - past, present, and future. *Integr Biol (Camb)* 2013; 5(1): 48-65

Stupp R, Mason WP, Van den Bent MJ *et al*. Radiotherapy plus conventional and adjuvant temozolomide for glioblastoma. *N Eng J Med* 2005; 352: 987-96

Tamayo J, Kosaka PM, Ruz JJ, San Paulo Á, Calleja M. Biosensors based on nanomechanical systems. Chem Soc Rev 2013; 42(3): 1287-1311

Volkov D, Strack G, Halámek J, Katz E, Sokolov I. Atomic force microscopy study of immunosensor surface to scale down the size of ELISA-type sensors. *Nanotechnology* 2010; 21(14): 145503.

von Deimling A, Louis DN, Wiestler OD. Molecular pathways in the formation of gliomas. *Glia* 1995; 15: 328-338.

von Muhlen MG, Brault ND, Knudsen SM, Jiang S, Manalis SR. Label-Free Biomarker Sensing in Undiluted Serum with Suspended Microchannel Resonators. *Anal Chem* 2010; 82: 1905-1910

Wang J, Tham D, Wei W, Shin YS, Ma C, Ahmad H, Shi Q, Yu J, Levine RD, Heath JR. Quantitating cell-cell interaction functions with applications to glioblastoma multiforme cancer cells. *Nano Lett* 2012; 12(12): 6101-6106.

Watanabe K, Tachibana O, Sata K, Yonekawa Y, Kleihues P, Ohgaki H. Overexpression of the EGF receptor and p53 mutations are mutually exclusive in the evolution of primary and secondary glioblastomas. *Brain Pathol* 1996; 6: 217-223.

Westphal M, Hilt DC, Bortley E *et al.* A phase 3 trial of local chemotherapy with biodegradable carmustine (BCNU) wafers (Gliadel wafers) in patients with primary malignant glioma. *Neuro Oncol* 2003; 5: 79-88

Xu S, Liu GY. Nanometer-Scale Fabrication by Simultaneous Nanoshaving and Molecular Self-Assembly. *Langmuir* 1997; 13: 127–129

Yang YT, Callegari C, Feng XL, Ekinci KL, Roukes ML. Zeptogram-Scale Nanomechanical Mass Sensing. *Nano Lett* 2006; 6: 583-586

Zougagh M, Ríos A. Micro-electromechanical sensors in the analytical field. *Analyst* 2009; 134(7): 1274-1290